# Paradoxical role of AT-rich interactive domain 1A in restraining pancreatic carcinogenesis

**Short Title:** Arid1a plays a context-dependent role in PDAC by regulating DNA repair.

Sammy Ferri-Borgogno[1*], Sugata Barui[1*], Amberly McGee[1*], Tamara Griffiths[1], Pankaj K Singh[4], Cortt G Piett[2], Bidyut Ghosh[1], Sanchari Bhattacharyya[3], Aatur Singhi[5], Kith Pradhan[3], Amit Verma[3], Zac Nagel[2], Anirban Maitra[1#], Sonal Gupta[1#]

[1]Sheikh Ahmed Center for Pancreatic Cancer Research, University of Texas MD Anderson Cancer Center, Houston, TX; [2]Center for Radiation Sciences, Harvard University School of Public Health, Boston, MA; [3]Department of Medicine, Albert Einstein College of Medicine, Bronx, NY; [4]Department of Experimental Radiation Oncology, University of Texas MD Anderson Cancer Center, Houston, TX; [5]Department of Pathology, University of Pittsburgh Medical Center, Pittsburgh, PA.

*Authors contributed equally
#Corresponding authors

**Abbreviations:** ARID1A, AT-rich interactive domain 1A; EMT, epithelial–mesenchymal transition; GEM, genetically engineered mouse; GSEA, gene set enrichment analysis; IPMN, intraductal papillary mucinous neoplasms; PDAC, pancreatic ductal adeno carcinoma.

**Correspondence:** Anirban Maitra, Sheikh Ahmed Center for Pancreatic Cancer Research, Ph: 713-7450861, Email:amaitra@mdanderson.org; Sonal Gupta, Sheikh Ahmed Center for Pancreatic Cancer Research, UT MD Anderson Cancer Center, 6565 MD Anderson Blvd, Houston, TX 77030, USA; Ph: 713-7450831, Email:sgupta8@mdanderson.org

## Abstract

**Background & Aims:** ARID1A is postulated to be a tumor suppressor gene owing to loss-of-function mutations in human pancreatic ductal adenocarcinomas (PDAC). However, its role in pancreatic pathogenesis is not clear despite recent studies using genetically engineered mouse (GEM) models. We aimed at further understanding of its direct functional role in PDAC, using a combination of GEM model, PDAC cell lines.

**Methods:** Pancreas-specific mutant *Arid1a*-driven GEM model (*Ptf1a*-Cre;*Kras*$^{G12D}$;*Arid1a*$^{f/f}$ or "KAC") was generated by crossing *Ptf1a*-Cre;*Kras*$^{G12D}$ ("KC") mice with *Arid1a*$^{f/f}$ mice and characterized histologically with timed necropsies. *Arid1a* was also deleted using CRISPR-Cas9 system in established PDAC cell lines to study the immediate effects of Arid1a loss in isogenic models. Cells lines with or without Arid1a expression were developed from respective autochthonous PDAC GEM models, compared functionally using various culture assays, and subjected to RNA-sequencing for comparative gene expression analysis. DNA damage repair was analyzed in cultured cells using immunofluorescence and COMET assay.

**Results:** Arid1a is critical for early progression of mutant *Kras*-driven pre-malignant lesions into PDAC, as evident by lower Ki-67 and higher apoptosis staining in "KAC" as compared to "KC" mice. Enforced deletion of *Arid1a* in established PDAC cell lines caused suppression of cellular growth and migration, accompanied by compromised DNA damage repair. Despite early development of relatively indolent cystic precursor lesions called intraductal papillary mucinous neoplasms (IPMNs), a subset of "KAC" mice developed aggressive PDAC in later ages. PDAC cells obtained from older autochthonous "KAC" mice revealed epigenetic changes underlying the various compensatory mechanisms to overcome the growth suppressive effects of Arid1a loss.

**Conclusions:** Arid1a is an essential survival gene whose loss impairs cellular growth, and thus, its expression is critical during early stages of pancreatic tumorigenesis in mouse models.

**Keywords:** SWI/SNF; pancreatic cancer; DNA repair; mouse model

## Introduction

The mammalian SWI/SNF complexes are chromatin remodelers that regulate gene expression by evicting nucleosomes at gene promoters. SWI/SNF subunits, particularly AT-rich interactive domain 1 (encoded by the *ARID1A*), are known to be involved in transcriptional regulation, DNA replication and DNA damage repair[1]. Mutations, translocations and deletions in human cancers lead to defective SWI/SNF complex assembly and recruitment, abnormal gene silencing and tumor development[2, 3]. Recent large-scale and integrated multi-platform sequencing analyses of pancreatic cancer ductal adenocarcinoma (PDAC) have revealed *ARID1A* mutations in ~6% of cases[4], besides predominant somatic mutations of *KRAS*, *TP53*, *SMAD4* and *CDKN2A*. These predicted loss-of-function alterations has led to the prevailing assumption that *ARID1A* behaves as a classic tumor suppressor gene (TSG), likely demonstrating genetic cooperation with mutant *KRAS* in pancreatic tumorigenesis. In fact, several recent genetically engineered mouse (GEM) models have been developed, largely based on this premise, with the investigators generating mice with pancreas-specific *Arid1a* loss and mutant Kras expression[5-8]. Predominantly, these GEM models showed appearance of intraductal papillary mucinous neoplasms (IPMNs), a *bona fide* precursor lesion of PDAC, with only one study reporting progression to PDAC on the backdrop of IPMNs in 20% of these mice. This led the investigators to conclude that loss of *Arid1a* in the context of mutant *Kras* results in an IPMN – PDAC pathway to invasive cancer in the pancreas[5]. However, rather inexplicably, other studies have also shown that the rate of *ARID1A* mutation or loss of expression in human IPMN samples is substantially higher than in human PDAC samples[5, 7, 9, 10]. This stands in stark contrast to all of the well-established TSGs in PDAC (particularly *TP53*, *SMAD4* and *CDKN2A*), which consistently demonstrate an increasing frequency of abnormalities in the multistep progression from precursors to invasive cancer[4, 11]. In order to functionally address this paradox, we revisited the

role of *ARID1A* loss in multistep pancreatic carcinogenesis. Consistent with prior reports, pancreatic exocrine deletion of *Arid1a* in conjunction with mutant *Kras* expression led to an IPMN-predominant histology, alongside non-cystic pancreatic intraepithelial neoplasia (PanINs) precursor lesions. Surprisingly, the lesions arising in "KAC" mice demonstrate markedly reduced proliferative rate, in contrast to "KC" mice with retained Arid1a function. This growth suppression was phenocopied *ex vivo* in murine and human cell lines with CRISPR-induced deletion of *ARID1A*, accompanied by significant impairment in DNA damage response (DDR). A compensatory upregulation of the SWI/SNF homolog ARID1B is observed in *ARID1A* mutant cells, which albeit not rescuing the growth arrest or DDR defect, results in a "synthetic essentiality"[12], creating a requirement of sustained Arid1b expression for survival, a facet that can be exploited as a therapeutic target. In a subset of "KAC" mice, we eventually observe the development of aggressive PDAC, accompanied by deregulation of a diverse array of putative escape mechanisms, including Myc overexpression or low Trp53 expression. Our functional data establishes that ARID1A does not behave as a classic TSG, but rather, its loss within pancreatic precursors restrains progression, unless circumvented by one of several escape mechanisms. Our findings reconcile the observed discrepancy in rates of Arid1a loss between human IPMNs and PDAC, and identify several potential targetable opportunities in tumors with *ARID1A* mutations.

## MATERIALS AND METHODS

Detailed methods are described in the Supplementary Materials and Methods. Primary antibodies are listed in Supplementary Table 4. Primer Sequences are described in Supplementary Table 5.

### Genetically Engineered Mice

All mice experiments were approved by UT MD Anderson Institutional Animal Care and Use Committee (IACUC) and performed in accordance with the NIH guidelines for use and care of live animals under the protocol number 00001222-RN01. *LSL-KrasG12D*, *Ptf1a-Cre/+*, *ARID1A*$^{fl/fl}$ mice have been described before and were purchased from Jackson laboratories. Genotyping

PCR was performed from genomic DNA from tails using standard protocol of N-Extract kit (Sigma).

**Cell culture**

Murine "KPC" cell line was derived from a spontaneous tumor arising in a female *LSL-Kras*$^{G12D/+}$;*LSL-Trp53*$^{R172H/+}$;*Pdx-1-Cre* ("KPC") mouse; "KC" and "KAC" cell lines were isolated from spontaneous tumors arising in *LSL-Kras*$^{G12D/+}$;*Pdx-1-Cre* and *LSL-Kras*$^{G12D/+}$;*ARID1a*$^{fl/fl}$;*Ptf1a-Cre* mice, respectively and their epithelial origin confirmed by genomic PCR for Cre-mediated Kras recombination. Patient-derived low passage cell line Pa04 was cultured as described before[13]. Cells were maintained at 37°C in humidified 5% $CO_2$ incubator and cultured in DMEM (Sigma-Aldrich, Cat#D6429) supplemented with 2 mM L-glutamine (Sigma-Aldrich, Cat#G7513), 10% FBS (Sigma-Aldrich, Cat#F2442), and 100ug/ml Pen-Strep (Corning, Cat# 30002CI). All cell lines were tested routinely for mycoplasma contamination.

**ARID1A Deletion by CRISPR/Cas9**

sgRNA cassette was generated using the CRISPR design tool (http://crispr.mit.edu). The sequence of various sgRNAs were Mouse-Ex.2a sgRNA (GGTCCCTGTTGTTGCGAGTA), Mouse-Ex3a sgRNA (GCCCTGCTGGCCATACGCAC), Human-Ex1a sgRNA (GATCCCCGCTGTCTCGTCCG), Human-Ex1b sgRNA (TTGTTGGGCCCCTCCCGAGG). The sgRNAs were cloned into the pX459 (pSpCas9 (BB)-2A-Puro) plasmid vector (Addgene, Cat#62988). Mouse or human cell lines were transfected with the abovementioned plasmids using Lipofectamine 3000, and positive cells selected in the presence of 1.5 µg/ml puromycin.

**Determination of cell growth and morphology**

Cellular morphology and proliferation were assessed using Incucyte live cell imager (Sartorius) and images analysed with the IncuCyte HD software. Proliferation was measured through quantitative kinetic processing metrics derived from time-lapse image acquisition and presented as percentage of culture confluence over time. For experiments where cells underwent change in morphology due to effect of a drug, cells stably expressing the inert RFP in the nuclei (transfected

with IncuCyte NucLight Red Lentivirus Reagent; Essen Bioscience, Cat#4476) were used to perform quantitative kinetic metrics and evaluate proliferation, expressed as count/well.

**3D cultures for Colony formation**

Anchorage-independent growth assay in soft agar was performed as described before [13]. Briefly, cells were seeded at a density of 1000 cells/well in 12-well plates with drug treatments on the next day. After two weeks, plates were fixed and stained with 0.005% Crystal violet solution (Sigma-Aldrich, Cat#C6158), imaged with ChemiDoc scanner (Biorad) and colonies counted using ImageJ software. For spheroid cultures, log-phase cultures were seeded @ 1000 cells/well in ultra-low attachment, round-bottom 96 well plates (Corning Costar, cat #7007) and allowed to grow in $37^0$C humidified growth incubator for 7-10days. For growth inhibition assays, treatment with chemical inhibitors or corresponding vehicle control was done 24 hr after seeding and spheroid growth imaged using spheroid imaging protocol of the Gen5 Image software on Cytation 3 (Biotek) using 10X objective lens.

**Migration assay**

In 96-well plates (Essence Bioscience Image Lock, Cat#4379) of confluent cell culture, a central scratch-wound per well was made using the 96-pin WoundMaker (Essence BioScience, Cat#4493). Cells were grown for a further 24 hours and the recovery of the scratch-wound was analysed by taking images at 1 h intervals with the Incucyte Live-Cell Imaging System (Essence BioScience). The images were analysed with the IncuCyte HD software and the results presented in the form of relative wound densities and standard deviations for each time point. The Relative wound density (%) represents the cell density in the wound area expressed relative to that outside the wound area as a function of time.

**Immunofluorescent (IF) Staining for Foci Formation**

Twenty-four hours after seeding cells on IBIDI µ-Slides Collagen IV coated (IBIDI, Cat#80822), they were treated with 0.1uM of Doxorubicin (Doxo) (Sigma-Aldrich, Cat#D1515) for 30min. After media change, cells were grown for 0, 2, 4, 8 and 24h hours and then washed with DPBS (Sigma-

Aldrich Cat#D8537) and fixed with 4% Formalin (Sigma-Aldrich, Cat#HT5011) for 10min at RT. After washes, cells were Permeabilized with DPBS containing 0.5% Triton-X100 (Sigma-Aldrich, Cat#X100) for 10min at RT. Blocking was then performed with DBPS containing 3% BSA (Roche, Cat#3116956001) and 1% Chicken serum (Sigma-Aldrich, Cat#C5405) for 1 hour at RT and P-H2AX (1:800) and 53BP1 (1:1000) primary antibodies were incubated over night at 4C and secondary antibodies for 1 hour at room temperature. After DAPI staining, slides were mounted with mounting media (DAKO, Cat#S3023) and pictures taken using an Andor Revolution XDi WD Spinning Disk Confocal Microscope (Andor). Five different fields of pictures were taken for each well with same intensities and laser power for all cell lines. Images were then processed and analysed for quantification of foci/cell with iMaris 9.2 Image Analysis Software.

**Alkaline Comet assay**

Comet Assay was performed using the TREVIGEN CometAssay Kit (Cat#4250-050-K), according to manufacturer's instructions. Briefly, cells were seeded into 6-well plates and treated next day with 0.1uM of Doxorubicin for 30min. After media change, cells were cultured for 2 or 24h and then combined with molten LMAgarose (Trevigen, Cat#4250-0505-02) at a ratio of 1:10 and immediately spread onto both wells of a CometSlide (Trevigen, Cat#4250-050-03). Upon lysis with Lysis Solution (Trevigen, Cat#4250-050-01) and immersion in Alkaline Unwinding Solution (200mM NaOH, 1mM EDTA, pH>13), slides were then placed into the electrophoresis slide tray of the CometAssay ES Unit (Trevigen, Cat#4250-050-ES) covered with Alkaline Electrophoresis Solution (200mM NaOH, 1mM EDTA, pH>13). After electrophoresis, slides were washed, dried, stained with SYBR Gold (Thermo Fisher Scientific, Cat# S11494) and scanned using 10X objective with the Cytation 3 Cell Imaging Multi-Mode Reader (BioTek, Cat#CYT3MV). Each well was scanned using a 10X10 grid (100 images total), images processed and analysed using CometScore 2.0 to calculate % of DNA in tail and Tail length (μm).

**Statistical analysis**

Statistical analyses were performed (with GraphPad Prism 7) using the unpaired Student's t test with Welch's correction and two-way ANOVA with Sidak's post hoc test, as appropriate. For all experiments with error bars, S.D. was calculated to indicate the variation within each experiment and data, and values represent mean±S.D.

## RESULTS

### Loss of Arid1a restrains expansion and progression of Ras-induced pancreatic precursor lesions

Since *Arid1a* is a critical gene from the standpoint of embryonic development [14, 15], we conditionally deleted *Arid1a* in the pancreatic epithelial compartment by crossing *Ptf1a-Cre* [16] and *Arid1a*$^{fl/fl}$ mice [14] to derive *Arid1a*$^{fl/fl}$*;Ptf1a-Cre* ("AC") mice. These "AC" mice survived until euthanasia when 80 week-old, however, histology at 8-weeks showed parenchymal atrophy with fatty replacement accompanied by inflammation, characteristic of pancreatitis, followed by appearance of acinar to ductal metaplasia (ADM), dilated ducts, and microscopic cysts lined by mucinous epithelium at 16-weeks (**Supplementary Figure S1A**). Histology at 40-week showed additional fluid-filled macroscopic cysts, along with few focal low-grade PanINs (LG-PanINs) (**Supplementary Figure S1B**). Immunohistochemistry (IHC) confirmed lack of Arid1a expression in epithelium of "AC" mice (**Supplementary Figure S1C**). Next, *LSL-Kras*$^{G12D}$*;Arid1a*$^{fl/fl}$*;Ptf1a-Cre* ("KAC") mice were generated by crossing *Arid1a*$^{fl/fl}$*;Ptf1a-Cre* ("AC") mice with *Lox-stop-lox Kras*$^{G12D}$ mice[17]. Both "KAC" and littermate control "KC" mice (*LSL-Kras*$^{G12D}$*;Ptf1a-Cre*) were necropsied either at first sign of distress or at periodic age intervals to perform histological assessment of pancreatic pathology. Numerous groups have described the natural history of disease in "KC" mice, which show histological pancreatic lesions, similar to human ADM and LG-PanINs around 16 weeks of age. These lesions progress to high-grade PanINs (HG-PanINs) with age and infrequently (<10% of cases) to frank PDAC after 1 year. In stark contrast with "KC", necropsy of "KAC" mice revealed large fluid-filled cysts in "KAC" mice at 8 weeks, which increased in size and distribution with age (**Figure 1A-B**). Histological analysis of 8-weeks old pancreas

showed extensive parenchymal replacement by mucinous cysts resembling low-grade branched duct gastric type IPMN (LG-IPMN) in humans, admixed with LG-PanINs (**Figure 1A**). Pancreas at 8-20-weeks showed LG-IPMN, ADM and LG-PanINs adjacent to normal appearing parenchyma (**Figure 1A**). With progressing age (20-32 weeks), the average area comprising of normal parenchyma gradually decreased in "KAC" pancreas (20.6% at 8-10 weeks, 7.7% at 16-20 weeks, 3.4% at 24-28 weeks), mostly replaced by LG-IPMNs, LG-PanINs and ADM lesions (**Figure 1B)**. Lack of Arid1a expression in the precursor lesions arising in the "KAC" mice was confirmed by IHC (**Supplementary Figure S2A-B).** To assess the growth potential of precursor lesions in "KC" and "KAC" mice, we performed IHC for Ki-67 on age-matched pancreatic tissues. As expected in "KC" mice, an average of 40-50% of PanINs showed nuclear Ki-67 staining, in contrast with ~5% Ki-67 staining in both IPMNs and PanINs of "KAC" mice, indicating lower proliferative potential of these cells (**Figure 1C, Supplementary Figure S2C)**. This lower proliferative state was complemented by a higher percentage of precursor lesions in "KAC" pancreata showing strong staining for cleaved caspase-3, indicating ongoing apoptosis in these cells **(Figure 1D,** *Early***; Supplementary Figure S2D,** *Late***)**. This suggested that Arid1a is critical for growth of pancreatic premalignant lesions during early stages of disease development.

Despite restrained growth of precursor lesions, we witnessed a discernible shift in mortality of "KAC" mice with subsequent age (**Figure 1E;** 84% survival at 32 weeks versus 48% at 38 weeks). Histological assessment of pancreatic tissue revealed appearance of isolated foci of well-differentiated PDAC surrounded by confluent areas of LG-IPMNs, scattered ADMs and LG-PanINs in 4/11 mice (**Figure 1F).** With progressing age, survival of "KAC" mice reduced further to 36%, accompanied by growth of unifocal PDAC in 18/30 "KAC" mice, which were topographically distinct from LG-IPMN, LG-PanINs and rest of pancreatic tissue. Most of these PDAC were well-differentiated and metastasized to liver and lung (**Figure 1G)**. Notably, in these older mice, PDAC were still accompanied by LG-IPMN and LG-PanINs, instead of high grade

precursor lesions, which was in stark contrast with stepwise progression of lesions with age from low- to high-grade PanINs in "KC" mice.

**Loss of ARID1A expression in human IPMNs with low-grade dysplasia**

Due to dominance of LG-IPMNs of gastric subtype in Arid1a-null "KAC" mice, we assessed for loss of expression of ARID1A by IHC in a collection of 53 human IPMN sections representing various histological subtypes and dysplasia grades. Notably, loss of ARID1A expression was restricted only to low grade IPMNs of gastric subtype (**Figure 2A-B, Supplementary Table 1)** in 10/53 of all cases (~19%), while it was uniformly retained in high-grade IPMNs of gastric, intestinal and pancreato-biliary subtypes. Indeed, the high-grade IPMNs had an even stronger intensity of nuclear ARID1A expression than seen in adjacent normal ductal epithelium, suggesting an ongoing requirement for Arid1a function, in order to manifest as dysplastic progression. Even in IPMNs cases with mixed histological grades, the low-grade epithelium lacked ARID1A expression while the region with progression to high-grade dysplasia retained strong expression (**Figure 2C**). These findings from human IPMNs supported our GEM model data that loss of Arid1a might paradoxically constrain the progression of low grade IPMNs into higher-grade lesions.

**Arid1a Loss is detrimental to the growth of established PDAC lines**

To assess the direct functional role of Arid1a without other compensatory molecular events appearing during autochthonous progression in the "KAC" GEM model, we employed CRISPR-Cas9 based approach to delete this gene in the Arid1a-expressing PDAC lines established from "KC" and "KPC" mice. To this end, "KC" and "KPC" cells were transfected with two independent CRISPR-Cas9 sgRNAs plasmids, targeting exons 2 and 3 of the murine *Arid1a* gene, respectively. Genomic PCR sequencing and immunoblot analysis in CRISPR-ARID1A cells confirmed *Arid1a* deletion in puromycin-selected clones (**Supplementary Fig. S3A and Figure 3A**). Although CRISPR-ARID1A cells did not show any changes in cellular morphology (**Supplementary Fig. S3B**), they were both significantly growth retarded in monolayer cultures ("KC" and "KPC" CRISPR-ARID1A cells showed 70% and 50% reduced cell growth, respectively;

P<0.0001; **Figure 3B**). Similarly, both "KC" and "KPC" CRISPR-ARID1A cells showed greater than 50% decrease in number of anchorage-independent colonies with 14-day culture in soft agar (**Figure 3C-D,** P<0.01). Cell cycle analysis showed that *Arid1a* deletion caused significant G1 arrest in both "KC" and "KPC" cells (**Figure 3E**). This growth defect of CRISPR-ARID1A in both "KPC" and "KC" cells was more conspicuous in an orthotopic mouse model, where no macroscopic tumor was visible 7 weeks after implantation (**Figure 3F, "KPC"**). Histological analyses by H&E and IHC staining for ARID1A and Ki-67 confirmed absence of any ARID1A-negative PDAC cells in the residual pancreatic tissue and the only proliferating PDAC cells were ones that escaped *Arid1a* deletion (**Figure 3G**). To extend our findings from mouse model to human cells, we screened a panel of patient-derived low passage PDAC cell lines for ARID1A expression (**Figure 3H**) and deleted *ARID1A* in high ARID1A-expressing Pa04 cells, using CRISPR-Cas9 sgRNAs targeting two distinct portions of human *ARID1A* exon 1 (**Figure 3I**). Similar to mouse lines, CRISPR-ARID1A Pa04 cells showed growth retardation in both 2D and 3D growth assays compared to vector control (**Figure 3J-K; Supplementary Fig. S3C**).

To characterize autochthonous *Arid1a*-null IPMN cells, we attempted to establish cell lines from "KAC" mice with only IPMN lesions. Notably, these cells failed to grow stably in culture despite repeated attempts, consistent with our observed low Ki-67 staining and thus, low proliferative potential of *Arid1a*-null cells in vivo. However, we were able to establish PDAC cell lines from an autochthonous primary tumor (""KAC"-P") and the matched liver metastasis (""KAC"-L") from a 12-month old "KAC" mouse with invasive cancer. For subsequent experiments, we also used the aforementioned parental "KC" and "KPC" lines as orthogonal controls for "conventional" PDAC. Growth characteristics of these cell lines were compared in both 2D monolayer cultures and 3D aggregates in soft agar. While "KC" and "KPC" cells grew in clustered colonies with tight cell–cell adhesion, both autochthonous "KAC" lines showed elongated, spindle-shaped morphologies, characteristic of mesenchymal cells (**Figure 4A**). Gene expression analysis by semi-quantitative $RT^2$-PCR showed increased expression of epithelial–mesenchymal transition (EMT)-associated

genes in "KAC" cells (**Supplementary Fig. S4A**). Despite the difference in morphology, there was no significant difference in growth of the autochthonous "KAC" cells with "KC" or "KPC" cells, in either 2D or 3D cultures (**Figure 4B-C**), consistent with no difference in cell cycle progression between these lines (**Supplementary Fig. S4B**). To assess their *in vivo* growth characteristics, we implanted "KC", "KAC-P" and "KAC-L" cells orthotopically in the pancreas of athymic nude mice. Necropsy at 4 weeks post-injection showed no significant differences in the size of primary tumors among the groups at the macroscopic (data not shown) or microscopic levels, mirroring the well-differentiated grade of parental tumors (**Supplementary Fig. S4C).** In contrast with these autochthonous cell lines, the CRISPR-ARID1A derivatives of both "KPC" and "KC" cells showed reduced expression of EMT-associated genes (**Supplementary Fig. S3D**) and reduced migration, compared to the control cells (**Supplementary Fig. S3E-F**).

**Identification of candidate "escaper" mechanisms in autochthonous *Arid1a*-null PDAC cells**

To elucidate potential "escaper" mechanisms that might allow autochthonous *Arid1a*-null "KAC-P" cells to circumvent the growth constraining effects of Arid1a loss, and progress to PDAC, we subjected the RNA from "KAC-P" and "KC" cells to global RNA sequencing (RNA-Seq). Among all differentially expressed transcripts ($P<0.05$), 2560 genes were upregulated and 2660 genes were downregulated at least 2-fold in "KAC"-P cells compared to "KC" cells, with Claudin 18 (Cldn18) being one of the highest differentially-expressed transcripts (**Figure 4D, Supplementary Table 2**). Interestingly, CLDN18 has been reported to be expressed in larger percentage of precursor lesions and indolent neoplasms, like PanINs and IPMNs, than in PDAC[18]. We confirmed high Cldn18 expression at protein level in the autochthonous "KAC" lines, compared to "KC" and "KPC" cells (**Figure 4E**). Further, IHC on murine pancreatic tissues from "KAC" pancreases revealed robust expression in IPMN, PanIN and PDAC lesions (**Figure 4F**). We also found strong CLDN18 expression in *ARID1A*-negative human PDAC tissues; stressing the inverse correlation between the expressions of these proteins (**Figure 4G)**. To elucidate

whether *CLDN18* transcription is directly altered via changes in chromatin accessibility upon *Arid1a* loss, we generated *de novo* chromatin accessibility maps by performing ATAC-Seq in both "KC" and "KAC-P" cells. Data was validated by localization of ATAC-Seq peaks at known promoters and enhancers, available at ENCODE for the mouse genome, which confirmed the readily accessible chromatin surrounding the CLDN18 regulatory locus in "KAC-P" *versus* "KC" cells (**Figure 4H**). While we do not postulate CDN18 is an oncogenic "escaper" mechanism in "KAC" cells (especially as its upregulation is also seen in precursor lesions), our data identifies a facile membrane-based therapeutic target in human tumors with *ARID1A* mutations.

We performed gene set enrichment analysis (GSEA) of differentially expressed transcripts for known tumor-promoting networks that might serve as putative "escaper" mechanism(s) in "KAC-P" cells. GSEA identified enrichment of signatures positively associated with EMT (validated above, see **Supplementary Fig. S4A**), a positive association with Myc and E2F activity and negative association with p53 and Ras signaling in "KAC"-P" cells (**Figure 5A-B; Supplementary Fig. S4D**). We confirmed loss of Arid1a and p53 protein expression, and diminished expression of Cdkn1A/p21 (canonical p53 target), phospho-p44/42 MAPK (ERK1/2) and total ERK1/2 (downstream targets of oncogenic Kras signaling) in "KAC" lines, compared to "KC" control (**Figure 5C**, **Supplementary Fig. S4E**). Further, consistent with the Myc activation signature in "KAC-P" cells, we noted a substantial increase in levels of *TRP63* RNA and protein expression of ΔNp63α and γ isoforms in "KAC" cells compared to "KC" and "KPC" cells (**Figure 5C, Supplementary Fig. S4E**), which has been recently shown to positively regulate MYC function[19]. PDAC sections from the "KAC" mice also showed loss of p53 (**Figure 5D**) and strong MYC expression (**Figure 5E**), suggesting these as putative "escaper" mechanisms in the face of Arid1a loss. Parsing the RNA-Seq data, we identified pluripotency-associated transcription factors – Sox2 and Nanog – as significantly overexpressed in "KAC-P" cells (**Supplementary Table 2**) and confirmed high Sox2 expression and open promoter in "KAC" cells compared to control "KC" (**Figure 5F-G)**. Both transcription factors are aberrantly expressed in multiple cancers, including

PDAC[20-22] and believed to mark cancer stem cells and promote EMT[23], suggesting that transcription factors implicated in stem cell identity might also play a role in development of PDAC in "KAC" mice.

Thus, we found that loss of *Arid1a* in an oncogenic *Kras*-driven GEM model ("KAC") restricts proliferative potential and constrains histological progression of precursor lesions at early stages. Subsequently, PDAC develop in these mice due to a variety of candidate "escaper" mechanisms, likely under the selection pressure of oncogenic Ras.

**Impaired DNA damage repair as a potential mechanism restraining neoplastic progression in Arid1a null cells**

Reports in various solid cancers have shown that *ARID1A* mutations in cell lines are associated with compromised DNA damage repair, and enhanced sensitivity to agents inducing DNA double strand break (DSB), such as Cisplatin, or to the recently developed class of PARP inhibitors[24, 25]. Indeed, prior studies have shown that SWI/SNF complexes often localize to sites of DSBs and facilitate chromatin decondensation following serine 139 phosphorylation of histone H2AX (P-H2AX) via ATM/ATR[26]. To our surprise, however, RNA-Seq data comparing "KAC" *versus* "KC" cells showed enrichment of gene signatures associated with enhanced DNA repair in "KAC" cells (**Supplementary Fig. S5A)**. Underscoring this paradox, we found "KAC-P" cells to be relatively resistant to Cisplatin, compared to "KC" and "KPC" cells (**Supplementary Fig. S5B**). Similarly, contrary to other reports[25, 27], "KAC" and ARID1a-deleted isogenic "KC" and "KPC" cell lines were also resistant to ATR inhibitor, either alone or in context of DNA damage (**Supplementary Fig S5C-E)** or to various PARP inhibitors (data not shown). This led us to postulate whether in the compendium of potential "escaper" mechanisms that lead to emergence of cancers in "KAC" mice, overcoming an inherent DNA repair defect could also be one, thereby providing survival advantage to a subset of *Arid1a-null* cells, and a permissive milieu for progression to PDAC. To test this hypothesis, we assessed DNA repair competency upon immediate Arid1a deletion, mediated by CRISPR-Cas9 in "KPC" and "KC" cells. Doxorubicin (Doxo) is a well-known

chemotherapeutic agent known to induce DSBs and early activation of ATM leading to pH2AX and p53 activation[28]. Thus, pH2AX is an early and sensitive marker of DSB induction after Doxo treatment, when measured as foci by immunofluorescence[29], along with foci formation by DNA damage-responsive protein 53BP1, whose recruitment to DSBs is dependent on the protein platform assembled in pH2AX-positive foci[30]. We first measured nuclear foci of pH2AX and 53BP1 proteins in Doxo-treated isogenic "KPC" cells with and without ARID1A expression. Even at baseline, we found significantly reduced levels of pH2AX and 53BP1 foci in CRISPR-ARID1A compared to CRISPR-EMPTY cells (**Figure 6A and Supplementary Fig. S6A-B**). While control cells showed increased pH2AX and 53BP1-positive foci after 2 hours Doxo treatment (0.1μM), which came back to baseline state after 24 hours; the levels of foci in CRISPR-ARID1A cells were always significantly lower than control "KPC" cells, suggestive of an impaired DDR response. However, when assessed in the setting of wild type *TRP53* using isogenic "KC" cells, we did not find this decrease in the levels of either pH2AX or 53BP1 foci upon ARID1A deletion (**Figure 6B and Supplementary Fig. S6A-C;** "KC" CRISPR-EMPTY/ARID1A). For further evaluation of DNA damage and repair, we performed an orthogonal and highly sensitive comet assay, wherein quantification of the comet tail intensity relative to the head (% of DNA in tail) reflects the number of DNA breaks. Control cells from both "KPC" and "KC" cell lines (CRISPR-EMPTY) showed an initial increase of comets at 2h followed by reduction at 24h post-Doxo treatment, suggesting repair of damaged DNA (**Figure 6C-F**). In contrast, CRISPR-ARID1A cells from both lines showed higher amount of damaged DNA at 24h, indicative of impaired DDR capability (**Figure 6C-F**). This suggests that ARID1A is critical for DNA DSB repair, irrespective of active TRP53 signaling, but important for initial P-H2AX or 53BP1 foci formation in absence of active TRP53. Notably, confirming our premise of an "escaper" phenomenon in the "KAC" lines, while these cells had diminished levels of pH2AX or 53BP1 foci (**Supplementary Fig. S7A-C)**, reflecting their origin in the setting of *Arid1a* deficiency, they demonstrated comparable competency at post-Doxo DNA repair to both "KC" and "KPC" lines, as shown by Comet assay (**Supplementary Fig. S7D-E).**

**Loss of *Arid1a* causes impaired mismatch repair (MMR) in PDAC cells**

Recently, ARID1A was suggested to be important for DNA mismatch repair (MMR) due to its interaction with the MMR protein, MSH2 in ovarian and colon cancer cell lines[31]. Thus, we examined the direct role of ARID1A in MMR using the isogenic CRISPR-ARID1A "KC" and "KPC" cell lines. ARID1A loss in both "KC" and "KPC" lines showed compensatory increase in expression of MSH6, PMS2 and MLH1 proteins, suggestive of impaired MMR function and an ongoing requirement for the MMR machinery (**Figure 6G**). To confirm impaired MMR function, we utilized a quantitative functional MMR reporter assay[32] and found significantly reduced MMR capacity in the isogenic "KPC" line upon ARID1A deletion (**Figure 6H**). Interestingly, and in contrast to the discordance between autochthonous and isogenic lines observed with DSB repair, both the "KAC-P" and "KAC-L" cell lines also showed strong increase in expression of MSH6 and PMS2 proteins (**Figure 6I)**, and persistent functional impairment of MMR on the reporter assay ("KAC-P", $P<0.01$; "KAC-L", $P<0.05$) compared to "KC" and "KPC" cells (**Figure 6J**). Thus, impaired MMR in the setting of ARID1A loss appears to be a tumor neutral phenomenon that persists in the autochthonous lines. This is in contrast to the defective DSB repair that appears to be at least partially responsible for restraining neoplastic progression within the pancreatic epithelium, such that acquisition of competent DSB repair is observed in autochthonous lines that arise under selective pressure.

**Synthetic lethal targeting of Arid1a loss in PDAC**

The concept of synthetic lethality has been widely exploited for cancer therapy since most cancers have loss-of-function mutations that are not readily targetable. ARID1B, a structurally related but mutually exclusive homolog of ARID1A in the SWI/SNF chromatin-remodeling complex, is a potential synthetic lethal vulnerability in ARID1A-mutant human cancers[33]. Indeed loss of ARID1B in ARID1A-deficient cells destabilizes the SWI/SNF complex and impairs proliferation in gastric and ovarian cancers[34]. To explore this vulnerability in PDAC using our GEM model, we first confirmed the expression of ARID1B in ARID1A-null cell lines. Remarkably, both "KAC" lines and

isogenic lines with ARID1A deletion (CRISPR-ARID1A) showed increased expression of ARID1B, at both mRNA (**Figure 7A-B**) and protein level (**Figure 7C-D**), suggestive of a compensatory increase upon ARID1A loss. After confirming the successful knock down of Arid1b expression using short hairpin (pLK0-shARID1B) in both autochthonous and isogenic cells (**Figure 7C-D**), we found that only the "KAC" cell lines showed ≥ 80% decrease in cell proliferation, compared to "KC" or "KPC" control cells upon Arid1b knockdown (**Figure 7E**). Similarly, only ARID1A-null "KC" and "KPC" isogenic cell lines (CRISPR-ARID1A) showed reduction in cell proliferation compared to CRISPR-EMPTY control upon co-extinction of ARID1B (**Figure 7F**). The effect of Arid1b knockdown was also remarkable in reducing anchorage-independent growth of "KAC" cell lines in 3D cultures (~70% reduction in colony count; **Figure 7G** and **Supplementary Fig. S7A**). This indicates that ARID1B is a potential therapeutic target in ARID1A-deficient PDAC tumors, although currently there are no specific ARID1B inhibitors available for clinical trial. To overcome this concern, we explored other potential synthetic vulnerabilities of ARID1A-loss in our "KAC" model using commercially available small molecule inhibitors. Since MYC was one of the key "escaper" pathways upregulated in our "KAC" model, we tested the therapeutic vulnerability of "KAC" cells using 10058-F4, a specific small molecule inhibitor of MYC that prevents transactivation of MYC target gene expression[35]. In both monolayer and 3D spheroid cultures under ultralow-attachment conditions, "KAC" cell lines were significantly more vulnerable to 10058-F4 than control "KC" cells (**Figure 7H, Supplementary Fig. S7B)**. This "onco-dependence" suggests MYC activation to be, at least in part, critical for survival of "escaper" ARID1A-null cells. Recently, *Arid1a* mutation was reported as a biomarker for sensitivity of platinum-resistant urothelial carcinoma cells to Panobinostat-mediated HDAC targeting[36]. Interestingly, GSEA of gene expression data in these cells showed enrichment for MYC, E2F targets, and DNA repair pathways, similar to our observed GSEA data in "KAC" cells. This provided us with a strong rationale to test synthetic lethality of Panobinostat in our "KAC" PDAC model. Remarkably, compared to control "KC"/"KPC" cell lines, "KAC" cells showed significantly

better sensitivity to Panobinostat in both 2D monolayer cultures (**Figure 7I)** and 3D cultures for anchorage-independent growth (**Supplementary Fig S7C-D)**. Since Panobinostat is already a clinic-ready drug, this presents another potential opportunity for targeting *Arid1a*-null PDAC tumors.

HOMER analysis of our ATAC-Seq data showed enrichment in binding sites for PU.1 transcription factor in open chromatin regions of "KAC" compared to "KC" cells (**Supplementary Table 3**), suggesting higher functional activity of PU.1. Indeed, RNA-Seq and RT-PCR in the same population showed significant increase in levels of Csf1 (**Supplementary Fig S7E)**, which is a bona-fide target of PU.1. Using ENCODE database for mouse, we also found PU.1 binding sites in promoter of Cldn18, which was highly expressed in "KAC" cells (**Figure 5**). Utilizing a first-in-class small-molecule PU.1 inhibitor that specifically and allosterically interfere with PU.1-chromatin binding[37], we found "KAC" cells were significantly more sensitive in growth inhibition, compared to control "KC" and "KPC" cells (**Figure 7J)**, presenting PU.1 as another synthetic lethal target in ARID1A-null PDAC cells.

In summary, we identified a novel context-dependent role of Arid1a in PDAC where immediate loss of Arid1a function in cells is growth restrictive, at least partially due to impaired DNA repair, but potentially creates opportunities for various compensatory oncogenic mechanisms to drive the disease progression. We also identified therapeutic vulnerabilities of Arid1a-mutant PDAC cells that can be readily tested in clinical studies in imminent future.

## DISCUSSION

Deleterious mutations of *ARID1A* has been reported across multiple tumor types, resulting in the prevailing assumption that this *SWI/SNF* complex protein behaves as a prototypal tumor suppressor. However, DepMap analysis (https://depmap.org/portal/) of ARID1A using both CRISPR and RNAi screens in various cancer and pancreatic cancer cell lines showed dependency scores (CERES) <0, which indicates it is an essential gene for survival, as the score of -1 is comparable to the median of all pan-essential genes. Nonetheless, more nuanced

evidence from both functional and correlative data is emerging that suggest a reassessment of the role of *Arid1a* as a relatively straightforward TSG might be warranted. For example, Zhu and colleagues demonstrated in murine models of hepatocellular carcinomas (HCCs) that sustained Arid1a expression was pro-tumorigenic, while loss of Arid1a was deleterious, during primary tumor formation[38]. In contrast, loss of Arid1a was typically observed in "late-stage" metastatic HCC models, underscoring a context dependent role during multistep carcinogenesis. In fact, this and other studies[39] have shown that the vast majority of primary human HCCs (85-90%) retain Arid1a expression, at levels greater than the background liver, reiterating a need for sustained, and potentially enhanced Arid1a functional requirement, in early hepatocarcinogenesis. Similarly, in the context of intestinal neoplasia, concomitant bi-allelic deletion of Arid1a in the Apc$^{min}$ mice significantly inhibited tumor formation[40]. In addition, CRISPR-mediated deletion of *ARID1A* in human colorectal cancer cells with *KRAS* mutations significantly reduced proliferation, accompanied by attenuation of MEK/ERK dependent transcriptional signaling[41]. Conditional inactivation of *Arid1a* alleles in conjunction with *Apc* and *Pten* in the ovarian surface epithelium paradoxically prolonged survival of ovarian cancer-bearing mice and promoted the epithelial differentiation of resulting tumors[42]. *ARID1A* mutations also correlated with better survival in uterine corpus endometrial carcinoma[43]. Within same patients of endometrial cancer, primary tumors retained ARID1A expression, while metastatic subclones lost it due to deleterious mutations[44]. The sum total of these data brings into question the preconceived notion that *ARID1A* is a prototypal TSG independent of genetic context and/or disease stage.

Some of these apparently paradoxical data points have also begun to accumulate in PDAC, wherein the frequency of *ARID1A* genomic alterations is significantly higher in precursor IPMNs, and in particular, low grade IPMNs, than that in higher grade precursors or invasive adenocarcinomas. For example, in the TCGA analysis, only 6% of PDAC harbor somatic *ARID1A* alterations[4], while a recent single cell analysis of human IPMNs showed 40% with subclonal ARID1A mutations, all in the low-grade gastric type IPMNs[9]. In our own series, ~20% of patient

IPMN samples have complete loss of ARID1A protein expression by IHC (consistent with bi-allelic inactivation), all occurring in low-grade gastric type IPMNs. In the COSMIC database, well differentiated pancreatic neuroendocrine tumors, which are indolent tumors with a proliferation rate <3% Ki-67[45], carry a ~20% ARID1A mutation rate, more than three times higher frequency than the far more aggressive ductal adenocarcinomas (5.35%). Notably, these findings are in sharp contrast to well established TSGs, like *TRP53* and *CDKN2A*, which demonstrate a progressive increase in rate of alterations from low grade to high grade precursors to invasive adenocarcinoma[11], and where the frequency of mutations is typically higher in neoplasms at the aggressive end of the spectrum *versus* indolent tumors. These lines of evidence suggest that loss of Arid1a might not demonstrate outright genetic cooperation with oncogenic Ras in the pancreatic epithelium and thus warrant a careful reappraisal of the TSG role for *ARID1A* during multistep neoplastic progression ascribed in recently published GEM models[5-8].

Consistent with the published models, we found that *Ptf1a*-specific conditional loss of *Arid1a* in "*AC*" mice led to widespread pancreatitis and fatty replacement of post-mature parenchyma, suggesting that Arid1a is required for maintaining adult acinar homeostasis. This is comparable to conditional deletion of *Arid1a* leading to depletion of Lgr5-expressing mouse intestinal stem cells, disrupting intestinal homeostasis[46]. In mice with co-expression of mutant *Kras*$^{G12D}$ allele ("KAC"), the pancreas developed LG-IPMNs and LG-PanINs ubiquitously, with the former resembling gastric type IPMNs in patients, as has been previously reported[7, 8]. In contrast to "KC" mice, however, there was no stepwise progression of the LG precursors to HG precursor lesions, and the proliferative index (measured by nuclear Ki-67 labeling) was significantly (~10-fold) lower in the "KAC" pancreas, accompanied by a higher frequency of apoptotic nuclei. Surprisingly, only one other prior study has documented this low proliferation rate induced by *Arid1a* loss in pancreatic precursor lesions[5], albeit characterizing their IPMNs to be of pancreatobiliary- or oncocytic subtype, in contrast with gastric subtype reported by us and others. Consequently, we were unable to establish *in vitro* cell lines from the cystic precursors arising in the autochthonous

"KAC" mice, despite multiple attempts. However, paired cell lines established from a primary and metastatic PDAC lesion in the aged "KAC" mice, exhibited typical features of established cancer lines, including robust *in vivo* growth in orthotopic transplantation assays. Notably, these autochthonous "KAC" PDAC lines had complete loss of Arid1a expression, confirming their origin from successful *Cre*-mediated recombination. RNA-Seq followed by GSEA on these paired lines demonstrated several signaling nodes that were aberrant compared to "KC" cells, including downregulation of p53, and upregulation of MYC, and EMT- and pluripotency-associated transcription factors, respectively. Although, not formally tested in this study, MYC transcription has also been reported to be repressed by p53 and the loss of p53 synergistically enhancing the Myc–induced tumorigenesis[47]. The appearance of these highly ranked aberrant signaling nodes was not unexpected, since the prior studies in autochthonous models have also reported upregulation of EMT-associated genes[8] and MYC activation within the resulting *Arid1a*-null cancers[7] and low ARID1A expression significantly correlated with low Ki-67 labeling index and negative p53 expression in breast cancer patients[48]. One interesting facet that emerged from the GSEA was downregulation of Ras signaling in the "KAC" lines, which was confirmed by assessment of MAPK activity. In this context, while MYC is considered a downstream effector of oncogenic Ras in PDAC, mediating its pleiotropic effects on tumor cell growth and metabolism[49, 50], MYC can also substitute as a pivotal driver in the setting of "Ras independence", and the resulting tumors tend to be highly aggressive and chemoresistant[51, 52].

The isogenic CRISPR-ARID1A clones of "KC" and "KPC" cells, developed in present study, were strikingly different in their behavior from the autochthonous "KAC" PDAC lines, which can be postulated to arise through an "escape" phenomenon from *Arid1a* deletion-induced growth constraint *in vivo*, likely under the selection pressure of oncogenic Ras and other secondary events within the pancreatic epithelium. Further, the compendium of tumor-promoting pathways in the autochthonous PDAC models (such as Myc upregulation and perturbation of p53 function) identified by us, and others[5, 7, 8], are likely to be the molecular adaptations underlying this "escape"

phenomenon. It is worth noting that in at least one prior study[8], the "KAC" genotype rarely progressed to invasive cancers, with mice mostly developing IPMN precursors, unless additionally crossed to a mutant *Trp53* background (providing one prototypal "escape" mechanism). Similarly, our recently published CRISPR-based mouse model of PDAC[53] showed *Arid1a* loss concurrent with oncogenic *Kras* mutation in adult acinar tissue only caused LG-PanINs, while emergence of well-differentiated PDAC in the same period required deletion of *TRP53*, irrespective of Arid1a loss. The distinction between the two scenarios – whether Arid1a loss cooperates with oncogenic Ras to induce PDAC formation (as proposed[5-8]), or invasive cancers arise via an "escape" phenomenon in the setting of growth constrained precursors - goes beyond semantics, given the occurrence of *ARID1A* mutations across a multitude of epithelial pre-cancers[54].

What mechanism underlies the inability of *Arid1a*-deleted precursor lesions to robustly proliferate *in vivo*? Parsing the GSEA data on the "KAC" PDAC lines identified DNA repair as one of the highly ranked pathways, which was paradoxical, since numerous prior studies in preclinical models have suggested that the ARID1A protein (and other members of the BAF complex) is integral to repair of DNA DSBs[24-26, 55]. Specifically, Arid1a localizes to sites of DSBs through its interaction with DNA repair checkpoints, with loss of Arid1a leading to compromised homologous recombination repair (HR) and non-homologous end joining (NHEJ), the two major arms of DSB repair. Further, these studies have also shown increased sensitivity of cell lines with *ARID1A* mutations to DSB inducing agents like cisplatin, radiation and to PARP inhibitors[24, 25]. Surprisingly, our "KAC" cells were both relatively resistant to Cisplatin and PARP inhibitors (compared to the "KC" and "KPC" lines), and by the Comet assay, their DNA repair proficiency was comparable to these *Arid1a* wild type PDAC lines. This led us to postulate that acquisition of DNA repair capacity might be a crucial "escape" mechanism co-opted by "KAC" cells, and *vice versa*, impaired DNA repair a feature of *Arid1a* ablated precursors. We used the two CRISPR-ARID1A lines as a surrogate for assessing DNA repair capability, and found, indeed, that in response to doxorubicin-induced DSBs, both isogenic derivatives of "KC" and "KPC" cells had compromised DNA repair

on the Comet assay, compared to the respective parental controls. Interestingly, while the p53 status of the isogenic cells impacted the initial localization of pH2AX or 53BP1 to sites of DSBs, even the "KC" cells with wild type p53 demonstrated impaired DNA repair on the Comet assay. Extrapolating from these findings, we hypothesize that early PDAC precursors (LG-IPMNs and LG-PanINs), which retain p53 function, are nonetheless susceptible to impaired DNA repair in the face of *Arid1a* deletion. At the same time, there is likely to be an ongoing requirement for a competent DNA repair machinery in the "KAC" precursor lesions, given that mutant Ras is well-established for generating reactive oxygen species (ROS) and inducing a state of oxidative and genetic stress within the pancreatic epithelium[56, 57]. During the natural history of these mice, *Arid1a* null precursor lesions that are unable to adapt, either "stall" or undergo apoptosis, while clones that can re-functionalize their repair machinery through secondary adaptations (e.g., loss of p53 expression) retain the capacity for progression to PDAC. The association between *ARID1A* mutations and MMR defects has been previously documented, most commonly in colorectal cancers[58, 59]. Similar to our observed increase in expression of MMR proteins in setting of *Arid1a* loss, overexpression of MMR proteins, such as PMS2, has been shown to disrupt mammalian MMR function causing genetic instability[60]. However, it is very likely that the functional impairment of MMR observed in the setting of *Arid1a* deletion is not a barrier to tumor progression that requires an "escape" (in contrast to other DNA repair defects), as there was no significant difference between the autochthonous "KPC" lines or the isogenic CRSIPR-ARID1A cells.

Finally, an area of considerable translational potential is the opportunity to develop targeted therapies against PDAC harboring *ARID1A* mutations. In light of our observations above, it is imperative that putative targets be distinguished into those that *persist* in the established PDAC, *versus* those that are present in precursor lesions, but are *circumvented* in established PDAC because of "escape" from Arid1a loss-induced growth constraints. For example, we posit that "escape" mechanisms are the basis for our observation that synthetic lethal effects described in other *ARID1A* mutant solid cancer models, such as susceptibility to PARP inhibition and

cisplatin[24, 25, 55], or to commercially available EZH2 inhibitors[61-63], are absent in the autochthonous PDAC lines that have arisen in the setting of "escape". On the contrary, a striking "synthetic essentiality"[12] that is ubiquitously identified in the *Arid1a* mutant PDAC cells is the requirement of sustained ARID1B expression for survival. We observed increased expression of Arid1b in *Arid1a*-null cells irrespective of an "escape" setting (i.e., in both "KAC" cells and the CRISPR-isogenic cells), reiterating this is a compensatory effect directly related to *Arid1a* deletion. GeneHancer analysis [64] of Promoter/Enhancer region of *Arid1b* showed multiple binding sites for transcription factors such as MYC (11 sites), RUNX3 (25 sites), SOX6 (14 sites), FOXA1 (9 sites), and ZNF213 (7 sites). Interestingly, expression of these transcription factors were upregulated (**Supplementary Table 2,** RNA-Seq) and their binding sites associated with open chromatin, as identified by motif analysis of ATAC-seq data (**Supplementary Table 3**) in "KAC" cells and thus, could be responsible for direct transcriptional regulation of Arid1b. The functional data in the CRISPR-isogenic models suggest that while Arid1b is a synthetic essentiality in *Arid1a*-deleted cells, nevertheless, its compensatory upregulation is unable to rescue the observed impairment of DNA repair and proliferation, requiring additional events (upregulation of Myc, loss of p53, etc.) to occur for cancer progression *in vivo*. Another target whose expression appears to be inversely related to *Arid1a* levels is Claudin 18 (CLDN18) and parsing the ATAC-Seq in "KAC" cells demonstrated that the promoter/enhancer regions of both *ARID1B* and *CLDN18* are replete with binding sites for the Pu.1 (SPI1) transcription factor (for example, the *ARID1B* promoter/enhancer had as many as 18 binding sites for Pu.1). We believe that Pu.1 could be one of the pivotal transcription factors driving the compendium of transcriptional alterations that are directly related to *ARID1A* loss in the pancreatic epithelium, including the compensatory expression of the synthetic essential, albeit currently "undruggable" Arid1b protein. In this regard, our proof of concept data with a first-in-class Pu.1 small molecule inhibitor demonstrates robust growth inhibition in "KAC" cells, and pending future validation studies, this might represent a facile pharmacological strategy for targeting *ARID1A* mutant PDAC. Additionally, Panobinostat, a

potent pan-HDAC inhibitor, has been shown to cause growth arrest and apoptosis in cells from many cancer types including leukemia, by decreasing MYC expression and increasing expression of TRP53, CDKN1A (p21), DNA repair genes such as FANCG, FOXO3A, GADD45A, GADD45B, and GADD45G[65]. In ovarian cancer model, ARID1A loss inactivated the pro-apoptotic function of TRP53 by upregulating HDAC6, which directly deacetylated Lys120 of TRP53[66]. Thus, it was not surprising that Panobinostat was particularly effective against Arid1a-null "KAC" cells with elevated Myc signaling and decreased TRP53 and CDKN1A expression.

In conclusion, using a repertoire of GEM models, autochthonous and isogenic cell line models, we provide compelling evidence that *ARID1A* is not a prototypal TSG in PDAC pathogenesis. *Au contraire*, *ARID1A* loss induces a paradoxical growth constraint within the resulting low-grade cystic precursor lesions harboring mutant Ras, a finding we believe underlies the prolonged, indolent natural history of most gastric type IPMNs in patients. Loss of Arid1a compromises cellular DNA repair capability, which is likely compounded by the genotoxic stress of mutant Ras, leading to growth arrest and apoptosis. Eventually, through loss of p53, or upregulation of oncogenic networks like Myc or stem cell transcription factors, a subset of Arid1a-depleted precursor cells progress to frank adenocarcinomas. Our data reassesses the utility of therapeutic vulnerabilities previously described in other *ARID1A* mutant cancer models (e.g., DNA repair defects or microsatellite instability), in the setting of PDAC[24, 25, 55], while describing novel opportunities for targeting this class of cancers in the clinic.

**Acknowledgments**. Sincere thanks to Drs Mark Hurd and Jun Zhao at Sheikh Ahmed Center for Pancreatic Cancer Research for providing human archival tissues for histological analysis. We are also grateful to following MD Anderson Core facilities: Surgical Oncology Histology core for their service in fixed tissue embedding and ATGC Core for RNA-Seq.

**References**

1. Kadoch C, Hargreaves DC, Hodges C, et al. Proteomic and bioinformatic analysis of mammalian SWI/SNF complexes identifies extensive roles in human malignancy. Nat Genet 2013;45:592-601.
2. Kadoch C, Crabtree GR. Mammalian SWI/SNF chromatin remodeling complexes and cancer: Mechanistic insights gained from human genomics. Science Advances 2015;1.
3. Lu C, Allis CD. SWI/SNF complex in cancer. Nat Genet 2017;49:178-179.
4. Cancer Genome Atlas Research Network. Electronic address aadhe, Cancer Genome Atlas Research N. Integrated Genomic Characterization of Pancreatic Ductal Adenocarcinoma. Cancer Cell 2017;32:185-203 e13.
5. Kimura Y, Fukuda A, Ogawa S, et al. ARID1A Maintains Differentiation of Pancreatic Ductal Cells and Inhibits Development of Pancreatic Ductal Adenocarcinoma in Mice. Gastroenterology 2018;155:194-209 e2.
6. Livshits G, Alonso-Curbelo D, Morris JPt, et al. Arid1a restrains Kras-dependent changes in acinar cell identity. Elife 2018;7.
7. Wang SC, Nassour I, Xiao S, et al. SWI/SNF component ARID1A restrains pancreatic neoplasia formation. Gut 2019;68:1259-1270.
8. Wang W, Friedland SC, Guo B, et al. ARID1A, a SWI/SNF subunit, is critical to acinar cell homeostasis and regeneration and is a barrier to transformation and epithelial-mesenchymal transition in the pancreas. Gut 2019;68:1245-1258.
9. Kuboki Y, Fischer CG, Beleva Guthrie V, et al. Single-cell sequencing defines genetic heterogeneity in pancreatic cancer precursor lesions. J Pathol 2019;247:347-356.
10. Tan MC, Basturk O, Brannon AR, et al. GNAS and KRAS Mutations Define Separate Progression Pathways in Intraductal Papillary Mucinous Neoplasm-Associated Carcinoma. J Am Coll Surg 2015;220:845-854 e1.
11. Ying H, Dey P, Yao W, et al. Genetics and biology of pancreatic ductal adenocarcinoma. Genes Dev 2016;30:355-85.
12. Zhao D, DePinho RA. Synthetic essentiality: Targeting tumor suppressor deficiencies in cancer. Bioessays 2017;39.
13. Gupta S, Pramanik D, Mukherjee R, et al. Molecular determinants of retinoic acid sensitivity in pancreatic cancer. Clin Cancer Res 2012;18:280-9.
14. Gao X, Tate P, Hu P, et al. ES cell pluripotency and germ-layer formation require the SWI/SNF chromatin remodeling component BAF250a. Proc Natl Acad Sci U S A 2008;105:6656-61.
15. Lei I, Gao X, Sham MH, et al. SWI/SNF protein component BAF250a regulates cardiac progenitor cell differentiation by modulating chromatin accessibility during second heart field development. J Biol Chem 2012;287:24255-62.
16. Kawaguchi Y, Cooper B, Gannon M, et al. The role of the transcriptional regulator Ptf1a in converting intestinal to pancreatic progenitors. Nat Genet 2002;32:128-34.
17. Jackson EL, Willis N, Mercer K, et al. Analysis of lung tumor initiation and progression using conditional expression of oncogenic K-ras. Genes Dev 2001;15:3243-8.
18. Tanaka M, Shibahara J, Fukushima N, et al. Claudin-18 is an early-stage marker of pancreatic carcinogenesis. J Histochem Cytochem 2011;59:942-52.
19. Chen Y, Li Y, Peng Y, et al. DeltaNp63alpha down-regulates c-Myc modulator MM1 via E3 ligase HERC3 in the regulation of cell senescence. Cell Death Differ 2018;25:2118-2129.
20. Herreros-Villanueva M, Zhang JS, Koenig A, et al. SOX2 promotes dedifferentiation and imparts stem cell-like features to pancreatic cancer cells. Oncogenesis 2013;2:e61.
21. Jeter CR, Liu B, Lu Y, et al. NANOG reprograms prostate cancer cells to castration resistance via dynamically repressing and engaging the AR/FOXA1 signaling axis. Cell Discov 2016;2:16041.

22. Wen J, Park JY, Park KH, et al. Oct4 and Nanog expression is associated with early stages of pancreatic carcinogenesis. Pancreas 2010;39:622-6.
23. Mamun MA, Mannoor K, Cao J, et al. SOX2 in Cancer Stemness: Tumor Malignancy and Therapeutic Potentials. J Mol Cell Biol 2018.
24. Park Y, Chui MH, Suryo Rahmanto Y, et al. Loss of ARID1A in Tumor Cells Renders Selective Vulnerability to Combined Ionizing Radiation and PARP Inhibitor Therapy. Clin Cancer Res 2019.
25. Shen J, Peng Y, Wei L, et al. ARID1A Deficiency Impairs the DNA Damage Checkpoint and Sensitizes Cells to PARP Inhibitors. Cancer Discov 2015;5:752-67.
26. Park JH, Park EJ, Lee HS, et al. Mammalian SWI/SNF complexes facilitate DNA double-strand break repair by promoting gamma-H2AX induction. EMBO J 2006;25:3986-97.
27. Williamson CT, Miller R, Pemberton HN, et al. ATR inhibitors as a synthetic lethal therapy for tumours deficient in ARID1A. Nat Commun 2016;7:13837.
28. Kurz EU, Douglas P, Lees-Miller SP. Doxorubicin activates ATM-dependent phosphorylation of multiple downstream targets in part through the generation of reactive oxygen species. J Biol Chem 2004;279:53272-81.
29. Huelsenbeck SC, Schorr A, Roos WP, et al. Rac1 protein signaling is required for DNA damage response stimulated by topoisomerase II poisons. J Biol Chem 2012;287:38590-9.
30. Panier S, Boulton SJ. Double-strand break repair: 53BP1 comes into focus. Nat Rev Mol Cell Biol 2014;15:7-18.
31. Shen J, Ju Z, Zhao W, et al. ARID1A deficiency promotes mutability and potentiates therapeutic antitumor immunity unleashed by immune checkpoint blockade. Nat Med 2018;24:556-562.
32. Nagel ZD, Margulies CM, Chaim IA, et al. Multiplexed DNA repair assays for multiple lesions and multiple doses via transcription inhibition and transcriptional mutagenesis. Proc Natl Acad Sci U S A 2014;111:E1823-32.
33. Pulice JL, Kadoch C. Composition and Function of Mammalian SWI/SNF Chromatin Remodeling Complexes in Human Disease. Cold Spring Harb Symp Quant Biol 2016;81:53-60.
34. Helming KC, Wang X, Wilson BG, et al. ARID1B is a specific vulnerability in ARID1A-mutant cancers. Nat Med 2014;20:251-4.
35. Huang MJ, Cheng YC, Liu CR, et al. A small-molecule c-Myc inhibitor, 10058-F4, induces cell-cycle arrest, apoptosis, and myeloid differentiation of human acute myeloid leukemia. Exp Hematol 2006;34:1480-9.
36. Gupta S, Albertson DJ, Parnell TJ, et al. Histone Deacetylase Inhibition Has Targeted Clinical Benefit in ARID1A-Mutated Advanced Urothelial Carcinoma. Mol Cancer Ther 2019;18:185-195.
37. Antony-Debre I, Paul A, Leite J, et al. Pharmacological inhibition of the transcription factor PU.1 in leukemia. J Clin Invest 2017;127:4297-4313.
38. Sun X, Wang SC, Wei Y, et al. Arid1a Has Context-Dependent Oncogenic and Tumor Suppressor Functions in Liver Cancer. Cancer Cell 2018;33:151-152.
39. Zhao J, Chen J, Lin H, et al. The Clinicopathologic Significance of BAF250a (ARID1A) Expression in Hepatocellular Carcinoma. Pathol Oncol Res 2016;22:453-9.
40. Mathur R, Alver BH, San Roman AK, et al. ARID1A loss impairs enhancer-mediated gene regulation and drives colon cancer in mice. Nat Genet 2017;49:296-302.
41. Sen M, Wang X, Hamdan FH, et al. ARID1A facilitates KRAS signaling-regulated enhancer activity in an AP1-dependent manner in colorectal cancer cells. Clin Epigenetics 2019;11:92.

42. Zhai Y, Kuick R, Tipton C, et al. Arid1a inactivation in an Apc- and Pten-defective mouse ovarian cancer model enhances epithelial differentiation and prolongs survival. J Pathol 2016;238:21-30.
43. Kandoth C, McLellan MD, Vandin F, et al. Mutational landscape and significance across 12 major cancer types. Nature 2013;502:333-339.
44. Gibson WJ, Hoivik EA, Halle MK, et al. The genomic landscape and evolution of endometrial carcinoma progression and abdominopelvic metastasis. Nat Genet 2016;48:848-55.
45. de Wilde RF, Edil BH, Hruban RH, et al. Well-differentiated pancreatic neuroendocrine tumors: from genetics to therapy. Nat Rev Gastroenterol Hepatol 2012;9:199-208.
46. Hiramatsu Y, Fukuda A, Ogawa S, et al. Arid1a is essential for intestinal stem cells through Sox9 regulation. Proc Natl Acad Sci U S A 2019;116:1704-1713.
47. Ho JS, Ma W, Mao DY, et al. p53-Dependent transcriptional repression of c-myc is required for G1 cell cycle arrest. Mol Cell Biol 2005;25:7423-31.
48. Cho HD, Lee JE, Jung HY, et al. Loss of Tumor Suppressor ARID1A Protein Expression Correlates with Poor Prognosis in Patients with Primary Breast Cancer. J Breast Cancer 2015;18:339-46.
49. Santana-Codina N, Roeth AA, Zhang Y, et al. Oncogenic KRAS supports pancreatic cancer through regulation of nucleotide synthesis. Nat Commun 2018;9:4945.
50. Hayes TK, Neel NF, Hu C, et al. Long-Term ERK Inhibition in KRAS-Mutant Pancreatic Cancer Is Associated with MYC Degradation and Senescence-like Growth Suppression. Cancer Cell 2016;29:75-89.
51. Genovese G, Carugo A, Tepper J, et al. Synthetic vulnerabilities of mesenchymal subpopulations in pancreatic cancer. Nature 2017;542:362-366.
52. Farrell AS, Joly MM, Allen-Petersen BL, et al. MYC regulates ductal-neuroendocrine lineage plasticity in pancreatic ductal adenocarcinoma associated with poor outcome and chemoresistance. Nat Commun 2017;8:1728.
53. Ideno N, Yamaguchi H, Okumura T, et al. A pipeline for rapidly generating genetically engineered mouse models of pancreatic cancer using in vivo CRISPR-Cas9-mediated somatic recombination. Lab Invest 2019;99:1233-1244.
54. Hodges C, Kirkland JG, Crabtree GR. The Many Roles of BAF (mSWI/SNF) and PBAF Complexes in Cancer. Cold Spring Harb Perspect Med 2016;6.
55. Watanabe R, Ui A, Kanno S, et al. SWI/SNF factors required for cellular resistance to DNA damage include ARID1A and ARID1B and show interdependent protein stability. Cancer Res 2014;74:2465-75.
56. Storz P. KRas, ROS and the initiation of pancreatic cancer. Small GTPases 2017;8:38-42.
57. DeNicola GM, Karreth FA, Humpton TJ, et al. Oncogene-induced Nrf2 transcription promotes ROS detoxification and tumorigenesis. Nature 2011;475:106-9.
58. Ye J, Zhou Y, Weiser MR, et al. Immunohistochemical detection of ARID1A in colorectal carcinoma: loss of staining is associated with sporadic microsatellite unstable tumors with medullary histology and high TNM stage. Hum Pathol 2014;45:2430-6.
59. Chou A, Toon CW, Clarkson A, et al. Loss of ARID1A expression in colorectal carcinoma is strongly associated with mismatch repair deficiency. Hum Pathol 2014;45:1697-703.
60. Gibson SL, Narayanan L, Hegan DC, et al. Overexpression of the DNA mismatch repair factor, PMS2, confers hypermutability and DNA damage tolerance. Cancer Lett 2006;244:195-202.
61. Kim KH, Kim W, Howard TP, et al. SWI/SNF-mutant cancers depend on catalytic and non-catalytic activity of EZH2. Nat Med 2015;21:1491-6.
62. Bitler BG, Aird KM, Garipov A, et al. Synthetic lethality by targeting EZH2 methyltransferase activity in ARID1A-mutated cancers. Nat Med 2015;21:231-8.

63. McCabe MT, Ott HM, Ganji G, et al. EZH2 inhibition as a therapeutic strategy for lymphoma with EZH2-activating mutations. Nature 2012;492:108-12.
64. Fishilevich S, Nudel R, Rappaport N, et al. GeneHancer: genome-wide integration of enhancers and target genes in GeneCards. Database (Oxford) 2017;2017.
65. Scuto A, Kirschbaum M, Kowolik C, et al. The novel histone deacetylase inhibitor, LBH589, induces expression of DNA damage response genes and apoptosis in Ph- acute lymphoblastic leukemia cells. Blood 2008;111:5093-100.
66. Bitler BG, Wu S, Park PH, et al. ARID1A-mutated ovarian cancers depend on HDAC6 activity. Nat Cell Biol 2017;19:962-973.

## FIGURE LEGENDS

**Figure 1. Conditional loss of Arid1a in mouse pancreas restricts growth of Kras-driven early premalignant lesions. A-B,** Representative gross macroscopic images and H&E stained histological sections from “KC” and “KAC” pancreata at early ages showing normal parenchyma replaced by mucinous cysts resembling human IPMNs. Representative images from at least 7 mice per age group are shown. **C,** Quantification of immunohistochemical (IHC) staining for Ki-67 on pancreata from age-matched mice revealed lower percentage of proliferating PanINs lesions in “KAC” than “KC” group. For Ki67 quantification, % of Pos= (number of cells positive for Ki67 staining in PanINs)/(total number of cells in PanINs) from at least 5 mice per age group. **D,** IHC staining for cleaved caspase-3 on 28-week old pancreata from “KC” and “KAC” mice showed stronger and widespread staining in acini and precursor lesions of “KAC” mice. **E,** Kaplan-Meier survival curve for “KC” and “KAC” mice showing overall shorter median survival of “KAC” mice (38 weeks versus 58 weeks for “KC”) with P value of <0.0001 based on Log-rank (Mantel-Cox) test. **F,** Representative histopathological section from 4/11 42-weeks “KAC” mice characterized by foci of well-differentiated PDAC surrounded by areas of LG-IPMNs, ADMs and LG-PanINs. **G,** Representative gross necropsy image and H&E stained sections from 48-week “KAC” mice showing well-differentiated PDAC (Pancreas), which metastasized to liver and lung, although majority of pancreas was still populated by IPMN lesions (IPMN). Scale bar is 100u.

**Figure 2. Loss of ARID1A expression among human IPMN is mostly restricted to low-grade gastric subtype IPMN**. **A,** IHC staining for ARID1A on patient samples representing IPMNs of various subtypes and dysplasia grade revealed lost expression specifically in low-grade lesions of gastric subtype. **B**, Representative sections from human pancreas showing IHC staining for ARID1A in intestinal versus gastric subtype of IPMN and in high-grade versus low-grade dysplasia in the same section **(C)**. Scale bar is 100u.

**Figure 3. Arid1a loss is deleterious to growth in established PDAC cell lines**. **A,** Immunoblotting for ARID1A showed complete loss of expression in "KC" and "KPC" cell lines transfected with CRISPR/Cas9 targeting mouse *Arid1a*. **B,** Monolayer culture *in vitro* showed reduced proliferation in *Arid1a*-deleted "KC" and "KPC" isogenic cell lines, represented as measure of culture confluence. Images were captured every 2 hours using the live-imaging system (Incucyte ZOOM) and data are represented as mean±SD. ****, P< 0.0001 as determined by two-way ANOVA test. **C-D**, Anchorage-independent colony growth assay on soft agar showed reduced number of colonies in *Arid1a*-deleted KC and KPC isogenic cell lines. Representative pictures of colonies stained with crystal violet are shown and the bar graph shows the % of colonies relative to the CRISPR-EMPTY control for each cell line. **E,** Flow cytometric cell cycle analysis of PI-stained isogenic "KC" and "KPC" cell lines. Histogram indicates the mean of percentage of cells in each phase of the cell cycle from three independent experiments. **F,** Orthotopically implanted isogenic "KPC" cells showed lack of growth in *Arid1a*-deleted cohort 50d post implantation. Plot shows mean±SD of primary tumor volume measured with digital caliper. **G,** Representative images of H&E and IHC staining for ARID1A and Ki67 expression in sections from orthotopic tumors showed absence of growth of *Arid1*a-deleted cells. Scale bar is 100u. **H,** Immunoblotting for ARID1A in a panel of patient-derived human cell lines and confirming loss of expression by CRISPR-ARID1A in a cell line with endogenous expression (**I**). J, Monolayer culture *in vitro* showed reduced proliferation in *Arid1a*-deleted Pa04 cells, represented as measure of

culture confluence. Images were captured every 2 hours using the live-imaging system (Incucyte ZOOM) and data are represented as mean±SD. ****, P< 0.0001 as determined by two-way ANOVA test. **K,** Anchorage-independent colony growth assay on soft agar showed reduced number of colonies in *Arid1a*-deleted Pa04 cells, expressed as mean of total colonies/well. Representative findings from at least 3 independent experiments and data analyzed using the two-tailed unpaired Student's t test and considered significant if *, *P*< 0.05; **, *P*< 0.01; ***, *P*< 0.001; ****, *P*< 0.0001, unless otherwise specified.

**Figure 4. Characterization of autochthonous *Arid1a*-null PDAC cells from "KAC" mice. A,** *In vitro* monolayer cultures of "KC", "KAC-P", "KAC-L" and "KPC" cells revealed mesenchymal-like elongated morphology of "KAC" cells. Scale bars, 100 µm. **B-C,** Assessment of growth in both monolayer (B) as well as soft agar (C) showed no significant difference between "KAC" cells when compared to "KC" and "KPC". Representative images of crystal violet stained colonies from 3 independent experiments. **D,** Volcano plot of differentially expressed genes in "KAC-P" and "KC" cells, using RNA-Seq, showed Claudin 18 (CLDN18) as one of the top hit (n=3 ). **E,** Immunoblotting for mouse CLDN18 confirmed high expression levels in "KAC" PDAC cells compared to "KC" and "KPC". **F,** IHC on pancreatic sections from "KAC" mice showed strong expression in epithelium of IPMN, PanIN, and PDAC, correlative with lack of ARID1A expression. *Left*, low magnification (2x objective) view of pancreatic section, *Right*, high magnification view (20x objective, Scale bar is 100u). **G,** IHC on FFPE sections from human PDAC showed inverse relation between expression of ARID1A and CLDN18. Scale bar is 100u. **H,** High transcript levels of Cldn18 in RNA-Seq corresponded to open chromatin at 5` promoter region of *Cldn18* gene by ATAC-Seq on "KC and "KAPC-P" cells (n=3).

**Figure 5. Identification of oncogenic mechanisms in "KAC" PDAC cells. A-B,** Representative plots from GSEA analysis of differentially expressed genes (2-fold change) identified from RNA-seq on "KC" and "KPC-P" cells revealed positive enrichment in hallmark of

EMT and Myc target genes and negative enrichment in Kras dependency gene signature and hallmark P53 pathway. **C,** Immunoblotting on protein lysates from autochthonous mouse PDAC cell lines showed loss of ARID1A and TRP53 expression in "KAC" cells along with reduction in levels of CDKN1A (p21) and phospho-Erk1/2. While total MYC levels were unchanged in all lines, "KAC" cells showed high levels of Trp63 (δN) isoform γ as compared to "KC" and "KPC" cells. **D-E,** Representative microscopic images of IHC for TRP53 and MYC on PDAC sections from >1-yr old "KC" and "KAC" mice showed focal loss of p53 expression and strong expression of MYC in ARID1A-negative "KAC" group. Scale bar is 100u. F, High expression of pluripotency-associated transcription factor SOX2 in "KAC" cell lines was validated by both $RT^2$-PCR (top) and immunoblotting (bottom). **G,** High transcript levels of Sox2 in RNA-Seq corresponded to open chromatin at 5` promoter region of *Sox2* gene by ATAC-Seq on "KC and "KAPC-P" cells (n=3).

**Figure 6. Loss of Arid1a impairs DNA damage and mismatch repair. A-B,** Immunofluorescent staining for phospho-gH2AX in isogenic pair of "KPC" **(A)** or "KC" **(B)** cell lines transfected with either empty vector (E) or Arid1a-targeting CRISPR (A), and exposed to DNA damaging agent like 0.1uM Doxorubicin (Doxo) for 30min, then released for the indicated time points. Graph representative of 3 independent experiments, show the quantification of number of foci/cell performed with iMaris Microscopy Image Analysis Software (Bitplane) and showing lower number of p-gH2AX positive foci only in *Arid1a*-deleted "KPC" cells but not "KC" cohort. **C-F,** Comet assay using Doxo treated isogenic pairs of "KPC "(**C-D**) and "KC" (**E-F**) cells lines showed impaired DNA damage repair in *Arid1a*-deleted cohort of both pairs. Representative images (left panels) and scatter plots with quantification of the comet tail intensity relative to the head, expressed in % of DNA in tail (right panels) are shown. *two-tailed unpaired Student's t test against untreated sample, $two-tailed unpaired Student's t test against 2h timepoint. **G, I,** Immunoblotting for MMR proteins on lysates from isogenic **(G**) or autochthonous **(I)** cell lines, with or without *Arid1a*-deletion, revealed higher expression of MSH6 and PMS2 in *Arid1a*-deleted cells. **H, J,** A

fluorescence-based multiplex flow-cytometric host cell reactivation assay (FM-HCR) that measures the ability of cultured cells to repair plasmid reporters bearing mismatch, showed defective MMR in *Arid1a*-deleted cells, expressed as % of reporter expression. Three independent experiments were conducted and data represented as mean±SD and two-tailed unpaired Student's t test have been used for data analysis (unless otherwise indicated) and considered significant if *, $P< 0.05$; **, $P< 0.01$; ***, $P< 0.001$; ****, $P< 0.0001$, unless otherwise specified.

**Figure 7. Identification of synthetic lethality in autochthonous *Arid1a*-null PDAC cells. A-B**, Semi-quantitative $RT^2$ PCR revealed higher expression of Arid1b mRNA trasncripts in *Arid1a*-deleted autochthonous (A) and isogenic (B) cell lines, compared to "KC" or CRISPR-EMPTY control cells, respectively. **C- D,** Immunoblotting for ARID1B confirmed loss of expression in *Arid1a*-deleted autochthonous (**C**) and isogenic (D) cell lines after Arid1b knockdown using pLKO-shRNA. **E-F,** In vitro monolayer cultures of autochthonous (E) and isogenic "KC" and "KPC" (F) cell lines upon knockdown of Arid1b, showed significant reduction in proliferation, expressed as % of pLKO-shCTRL-transduced cells. **G,** Anchorage-independent colony growth assay on soft agar showed significant reduction in number of colonies upon Arid1b-knockdown, predominantly in *Arid1a*-deleted "KAC" cell lines. Bar graph shows the % of colonies, normalized on the pLKO-shCTRL for each cell line. **H-J**, In vitro monolayer cultures of autochthonous PDAC cell lines were treated with Myc-inhibitor 10058-F4 (H), Panobinostat (I) or Pu.1 Inhibitor (J) at indicated doses for 72h and their growth measured either as culture confluence (H) or cell count (I-J), normalized to vehicle-treated control. Images were captured every 2 hours using the live-imaging system (Incucyte ZOOM) and data plotted as mean±SD. Two-tailed unpaired Student's t test was used for data analysis (unless otherwise indicated) and considered significant if $P< 0.05$; **, $P< 0.01$; ***, $P< 0.001$; ****, $P< 0.0001$.

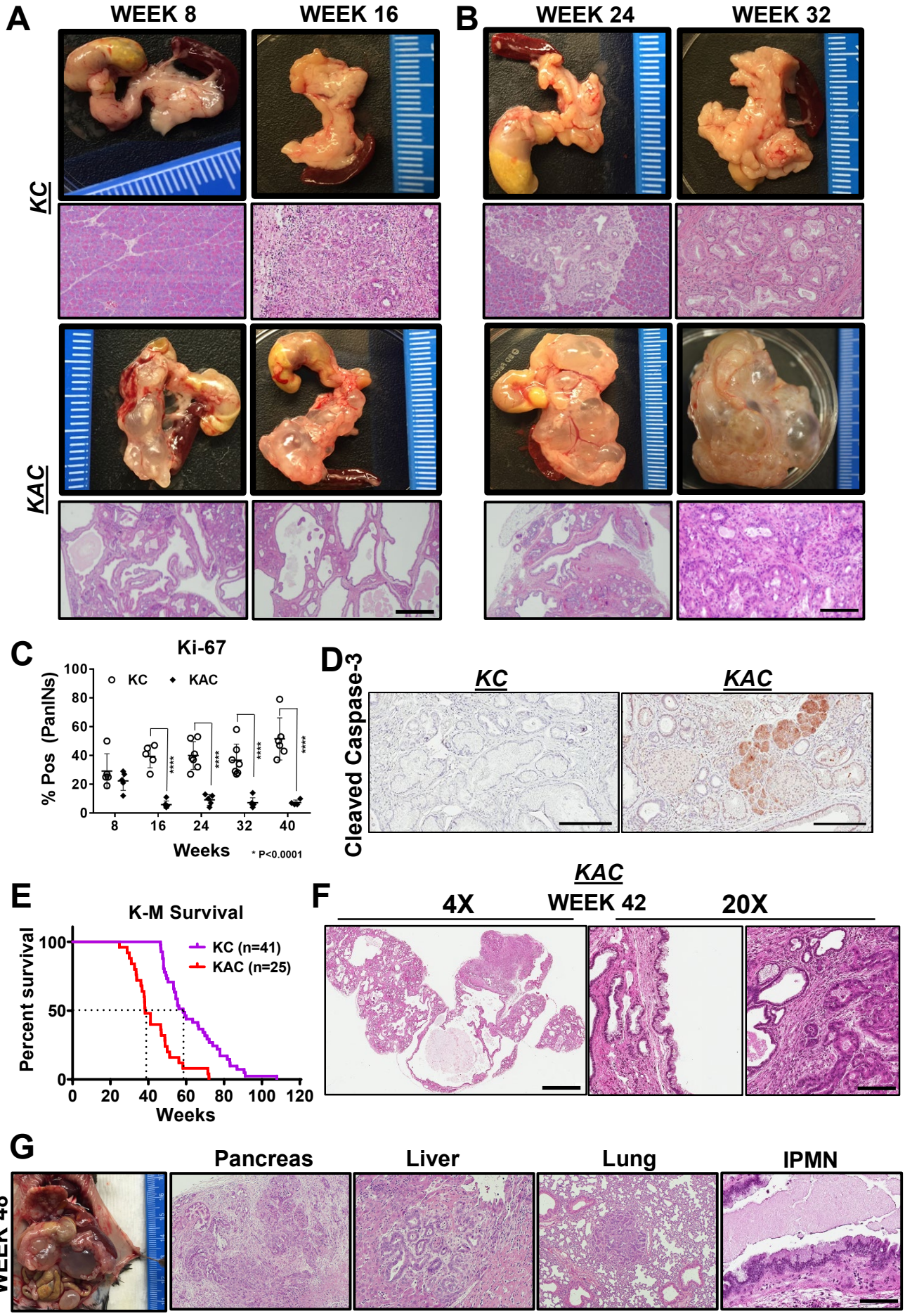


Figure 1

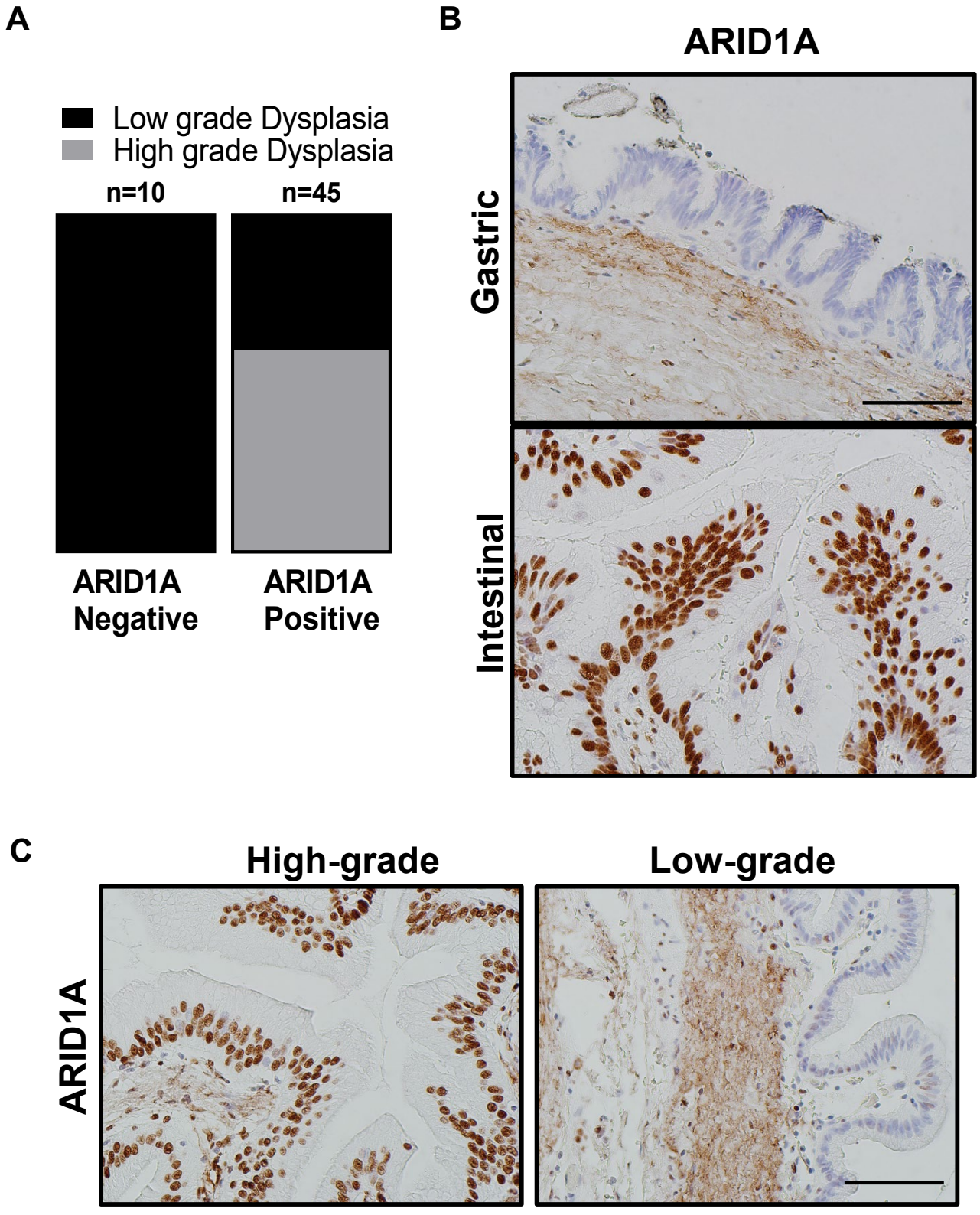


**Figure 2**

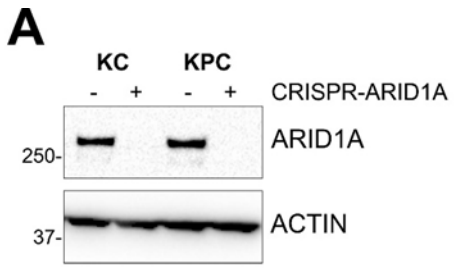


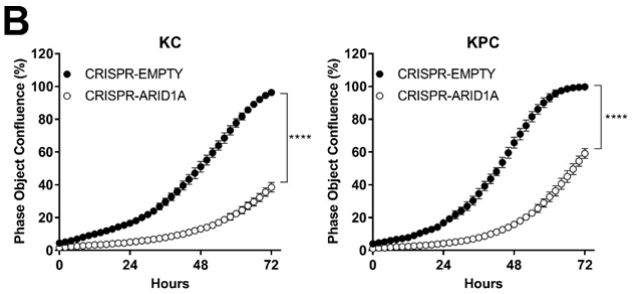


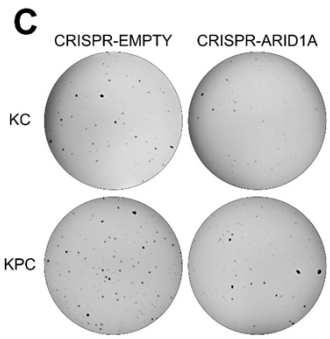


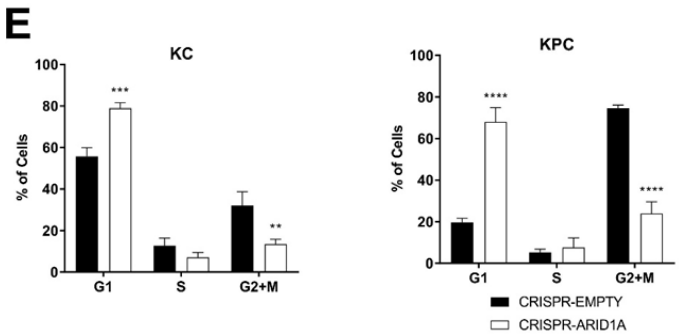


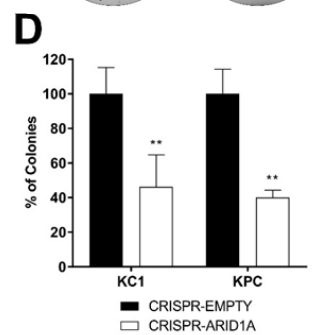


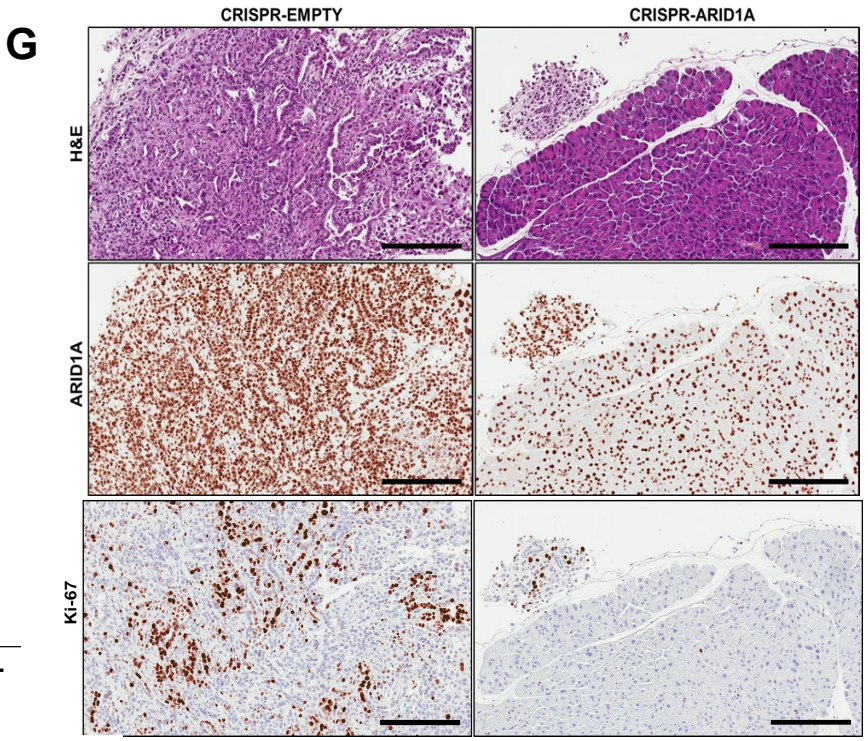


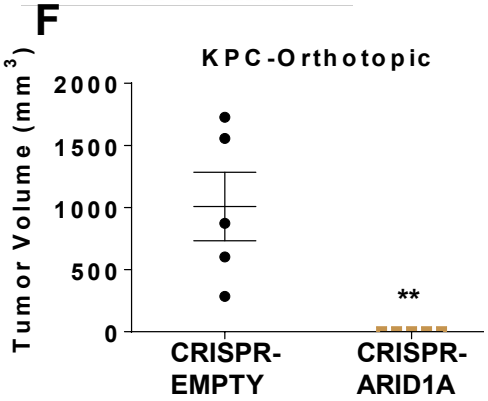


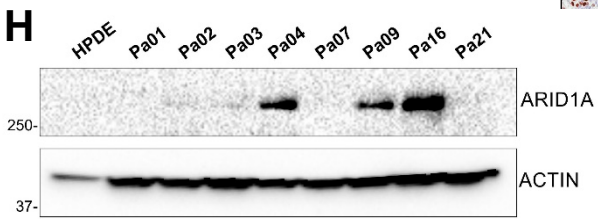


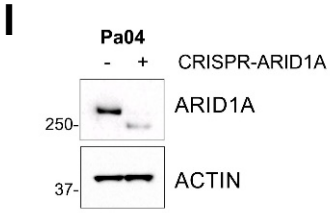


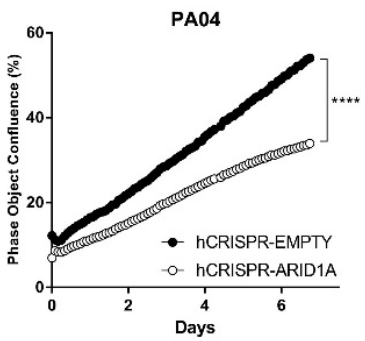


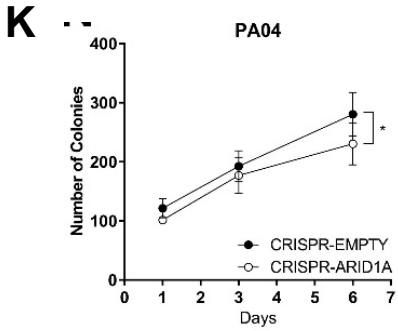


**Figure 3**

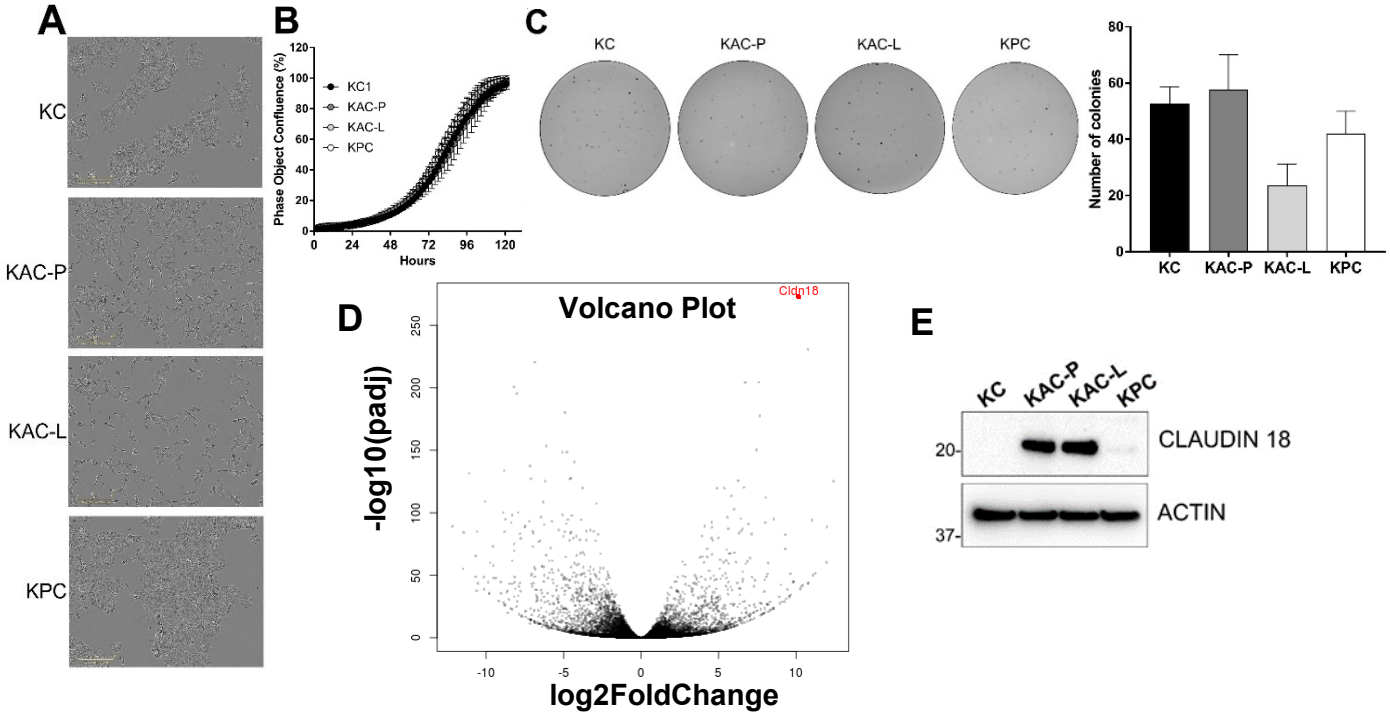


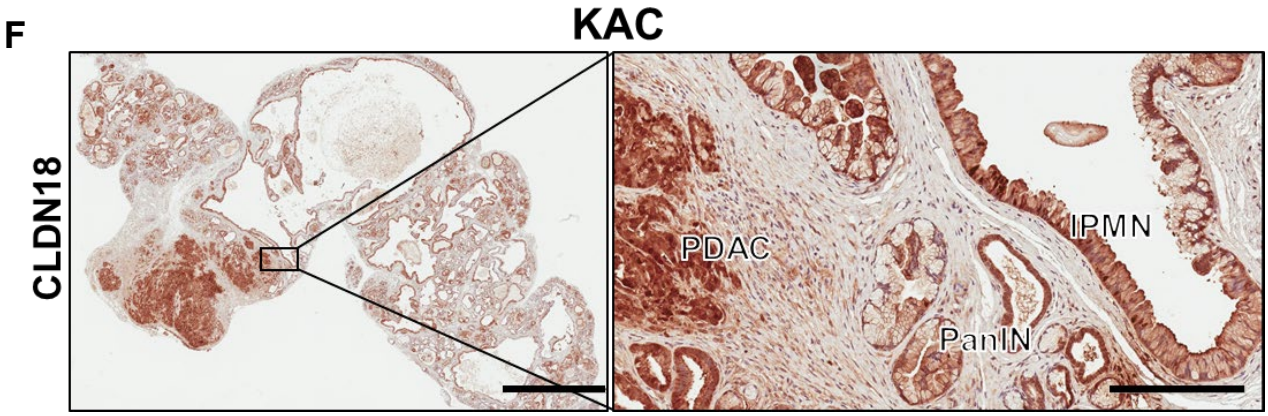


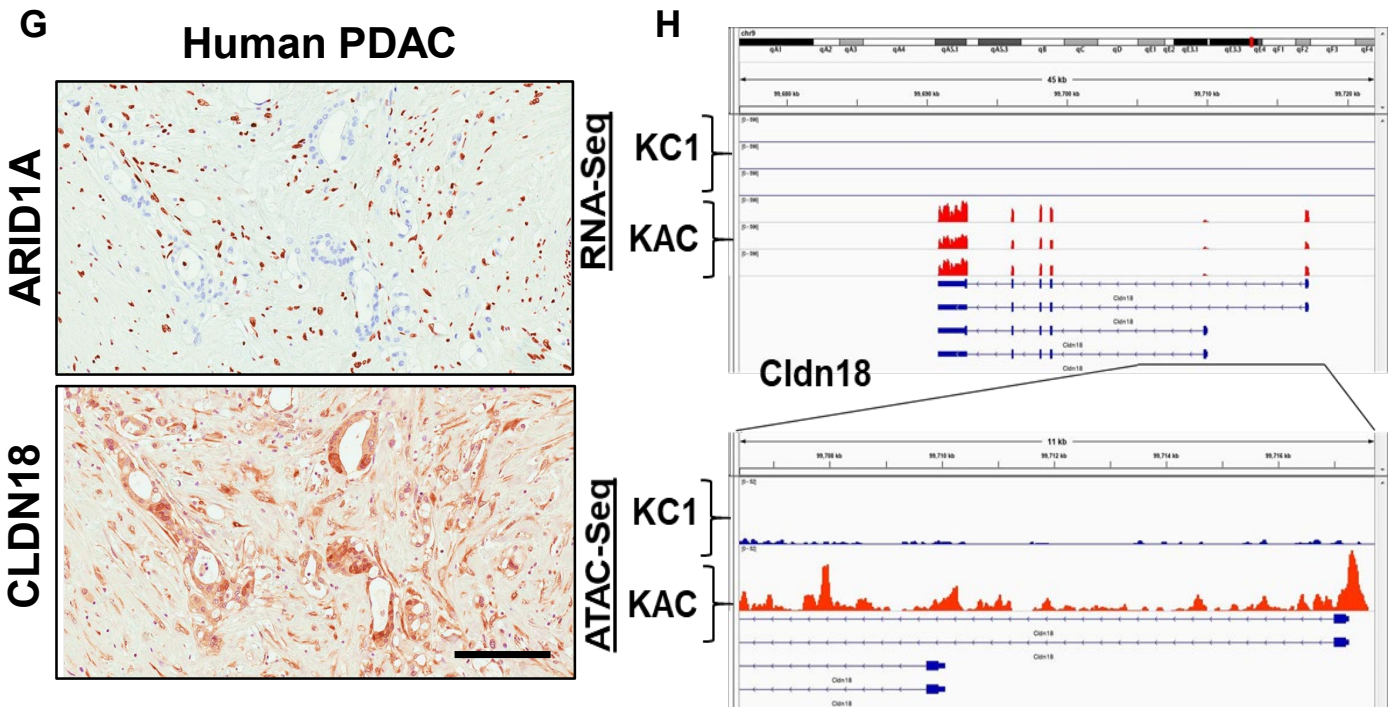


**Figure 4**

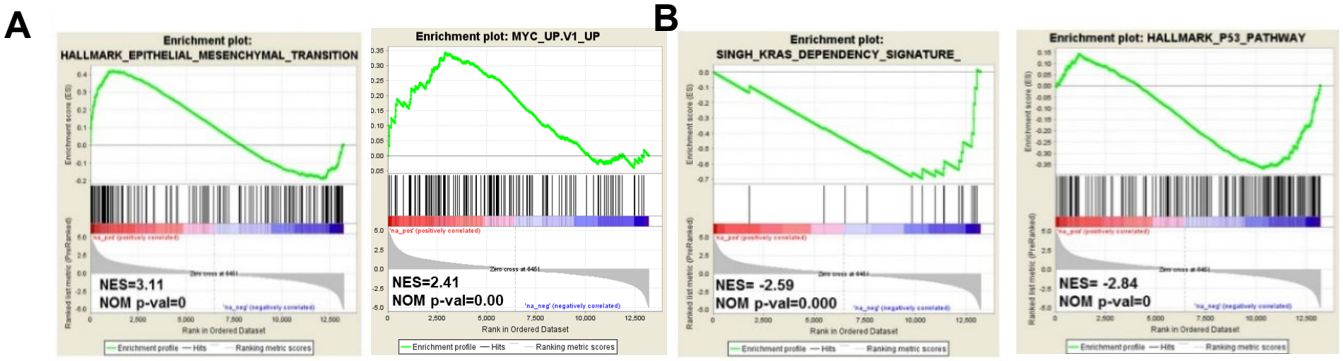


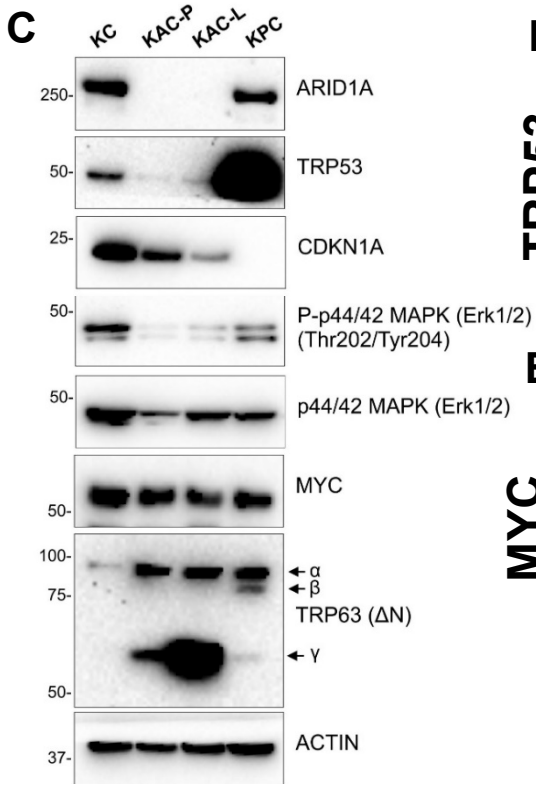


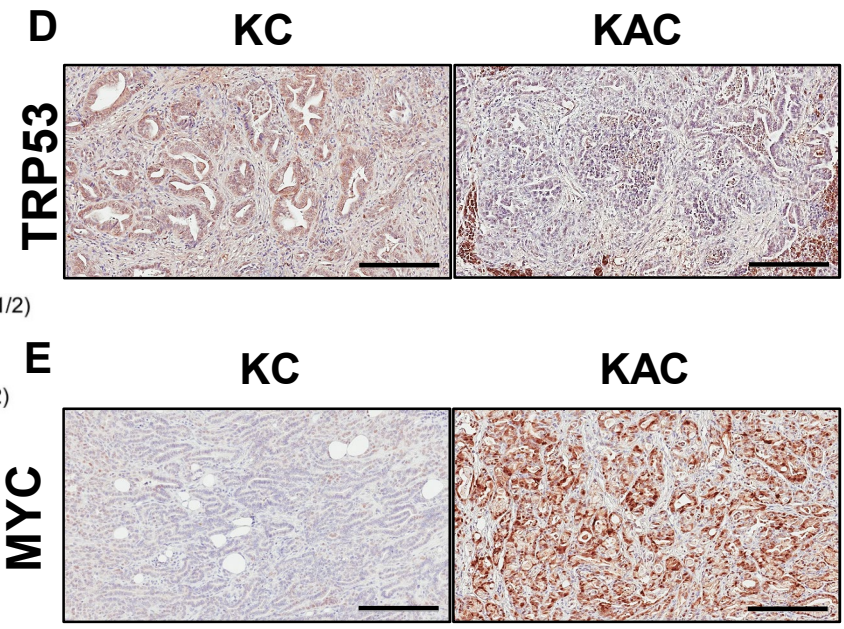


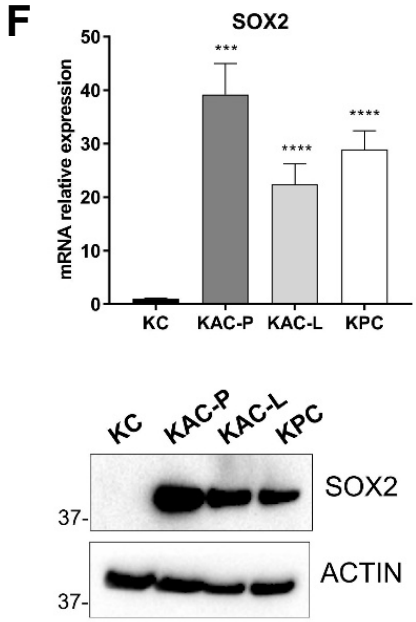


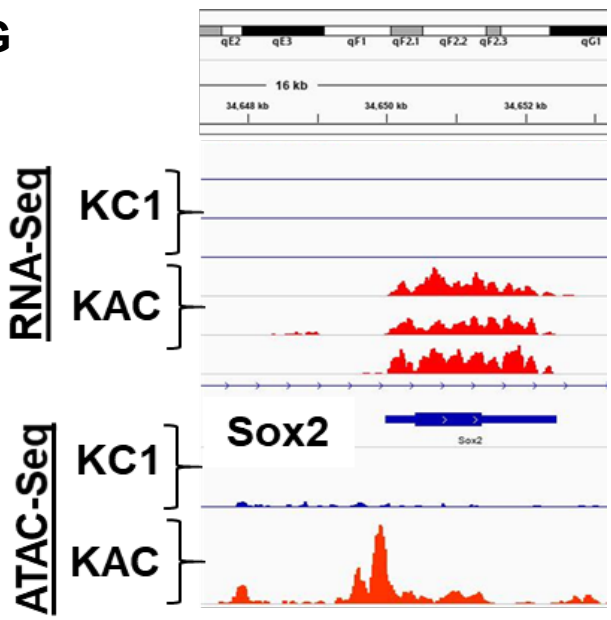


**Figure 5**

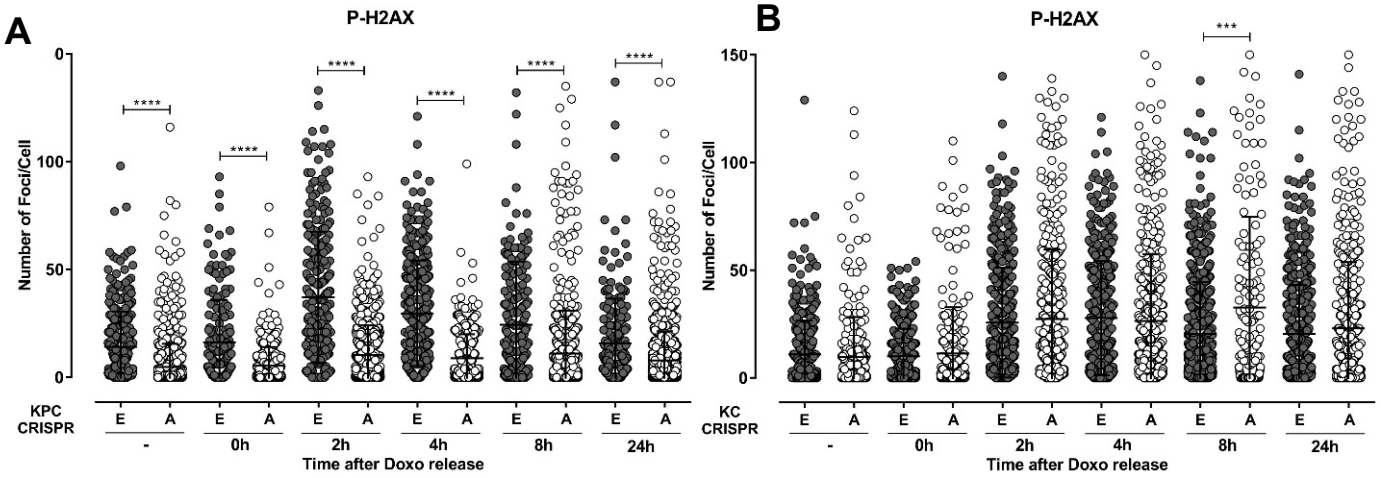


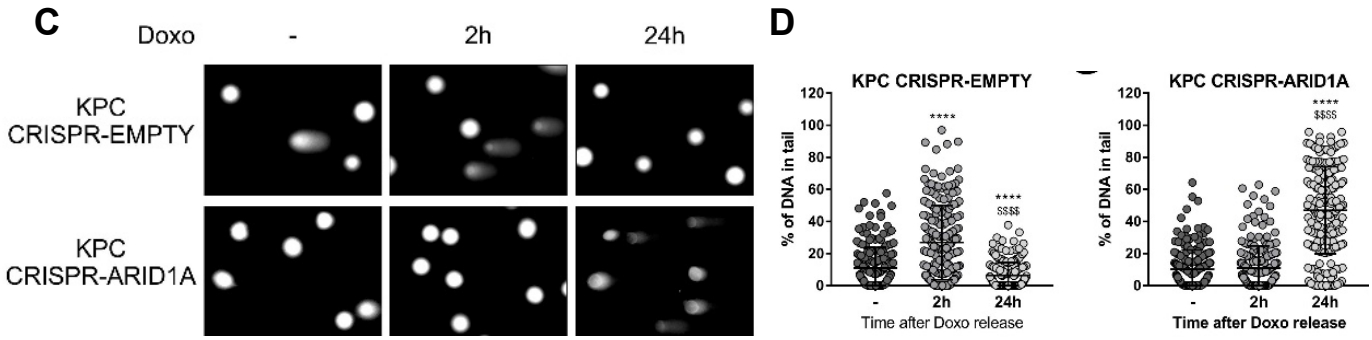


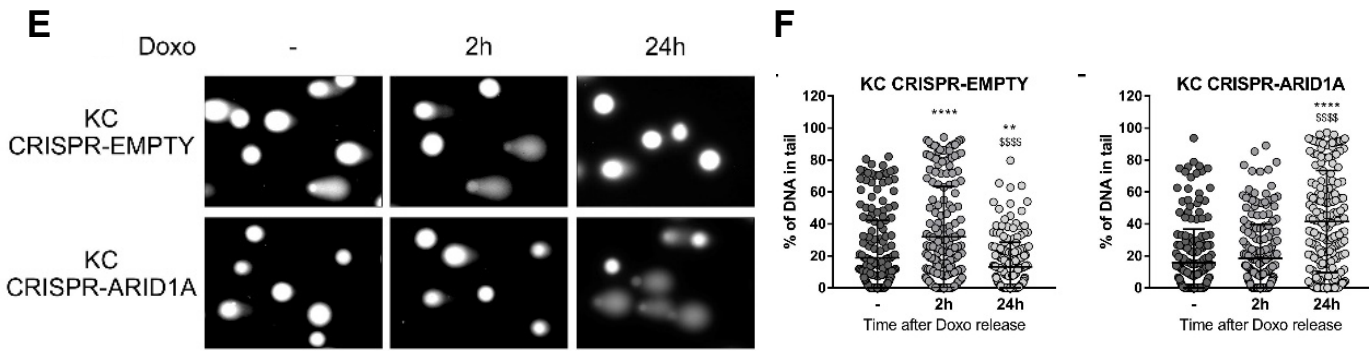


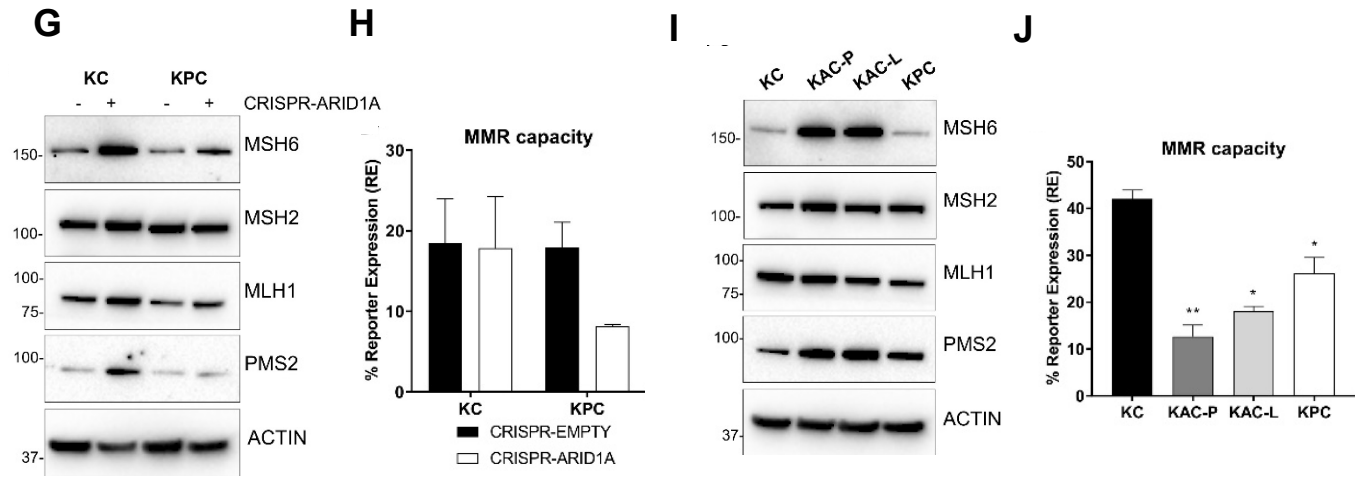


**Figure 6**

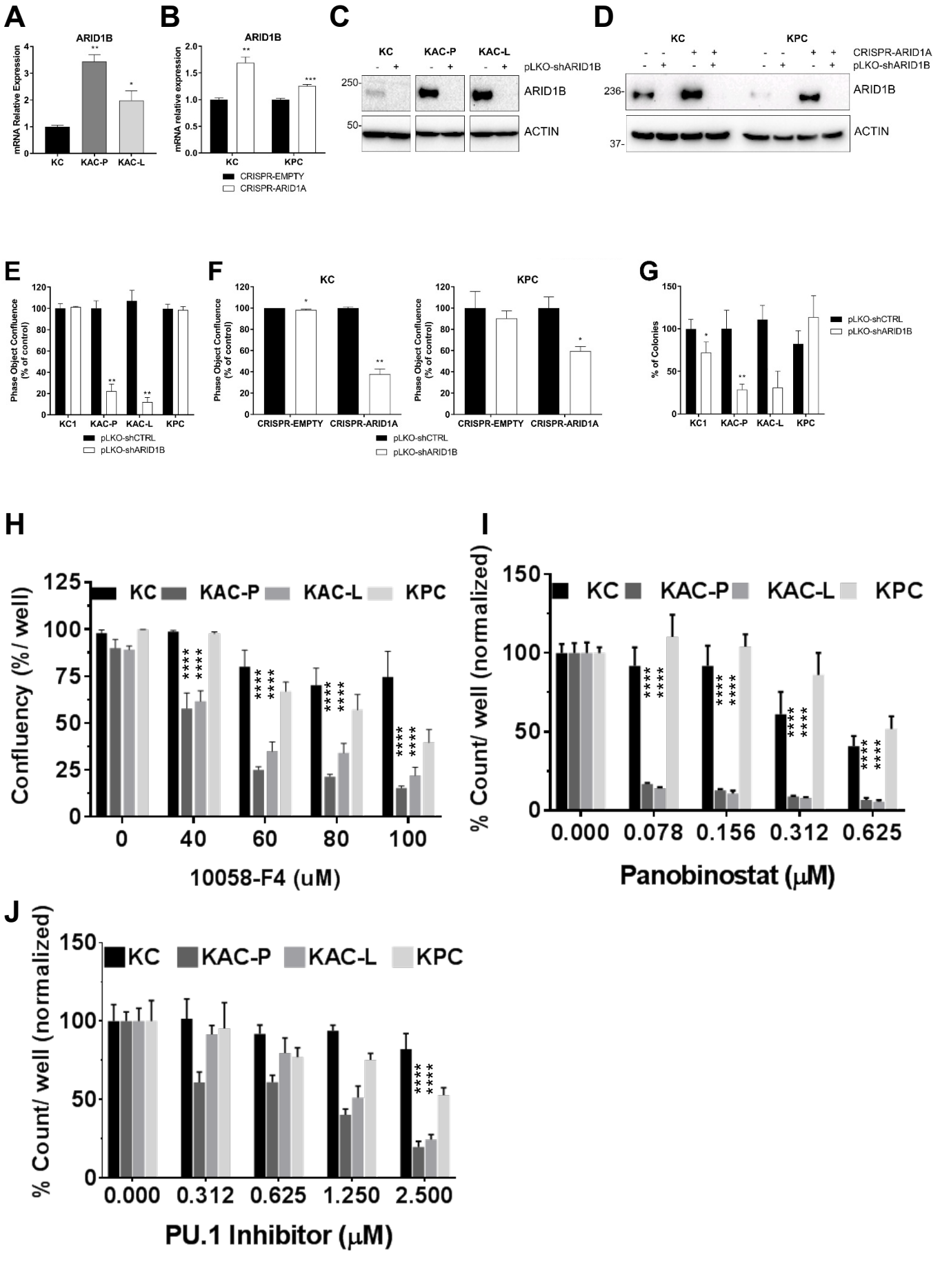


**Figure 7**